Indigenous Concrete Printer Technology: Future of Sustainable Construction

Submitted by

Raja Dilawar Riaz (G.L)

Ammar Ali

Usama Majid

Muhammad Faizan

Bachelor in civil engineering

Year (2019-2023)

Supervisor

Dr. Muhammad Usman

NUST Institute of Civil Engineering

School of Civil and Environmental Engineering

National University of Sciences and Technology, Islamabad, Pakistan

Indigenous Concrete Printer Technology: Future of Sustainable Construction

---

The Final Year Project Report

Presented to

SCHOOL OF CIVIL AND ENVIRONMENTAL ENGINEERING

NUST INSTITUTE OF CIVIL ENGINEERING

NUST

ISLAMABAD, PAKISTAN

In Partial Fulfillment

of the Requirements for the Degree of

Bachelor of Civil Engineering

---

by

Raja Dilawar Riaz (G.L)	297151
Ammar Ali	296648
Usama Majid	289280
Muhammad Faizan	296846

June 2023

CERTIFICATION

This is to certify that the thesis is titled

Indigenous Concrete Printer Technology: Future of Sustainable Construction

Submitted by

Raja Dilawar Riaz (G.L)	297151
Ammar Ali	296648
Usama Majid	289280
Muhammad Faizan	296846

Has been accepted towards the requirement.

for the undergraduate degree in

Civil Engineering

Dr. Muhammad Usman

Associate Professor

NUST Institute of Civil Engineering (NICE)

School of Civil and Environmental Engineering (SCEE)

National University of Sciences and Technology (NUST), Islamabad Pakistan

Acknowledgments

In the name of Allah, the Most Gracious and the Most Merciful Alhamdulillah, all praises to Allah for the strengths and His blessing in completing this project. Special appreciation goes to our supervisor, Dr. Muhammad Usman, for his supervision and constant support. His invaluable help of constructive comments and suggestions throughout the experimental and thesis works have contributed to the success of this project. Also special thanks to Brigadier Dr. Nasir Rasheed (Dean EME NUST) for his valuable support in the fabrication of concrete printers.

We are very thankful to "NICE - Structures Laboratory Staff" and "EME- RoboMak Laboratory Staff" for their support throughout the experimental work and they are highly appreciated. Also, we would like to express our gratitude to Bestway Cement Pvt. Ltd for their financial support in testing the mix design for concrete printing. We would also like to thank Pakistan Engineering Council (PEC) for generously funding this project.

We also offer my deepest feelings of gratitude to our friends and colleagues for their physical and moral support as well as encouragement which contributed a lot in making this entire research phase vigorous, motivating, and pleasant.

In the end, we are highly thankful to our parents. Their love, support, and prayers made us achieve this accomplishment.

Funding Acknowledgement

The research project titled “Indigenous Concrete Printer Technology: Future of Sustainable Construction” was successfully completed in the Structure Lab of NUST Institute of Civil Engineering (NICE), H12 Islamabad under the Pakistan Engineering Council (PEC) Annual Award of Final Year Design Projects (FYDPs) for the year 2022-23. The project was supervised by Dr. Muhammad Usman. We express our sincere gratitude to Dr. Muhammad Usman and the Pakistan Engineering Council for their invaluable financial support, which has significantly contributed to the progress and success of our project.

Dedication

We dedicate this research project to

Prof. Dr. Muhammad Usman, our mentor

And

Our Parents

Table of Contents

List of Figures

Gaussian Process Regressor model for different scenarios: (a) Casted Flexural Strength, (b) Printed Flexural Strength in Direction 1, (c) Printed Flexural Strength in Direction 2, and (d) Printed Tensile Strength of concrete. The curves visually demonstrate how well the model's predictions align with the actual values for each specific case, providing valuable insights into the model's performance for the different types of strength evaluation.

Figure 5.5 Graphical representation of the actual versus predicted results obtained from the XGBoost Regression model for different scenarios: (a) Casted Flexural Strength, (b) Printed Flexural Strength in Direction 1, (c) Printed Flexural Strength in Direction 2, and (d) Printed Tensile Strength of concrete. The curves visually demonstrate how well the model's predictions align with the actual values for each specific case, providing valuable insights into the model's performance for the different types of strength evaluation.

Figure 5.6 Comparison of the forecasted outcomes for different aspects of strength evaluation can be observed as follows: (a) Casted Flexural Strength (b) Printed Flexural Strength in Direction 1 (c) Printed Flexural Strength in Direction 2 (d) Printed Tensile Strength of Concrete.

List of Tables

Abstract

The construction industry is witnessing a paradigm shift with the integration of cutting-edge technologies, such as 3D concrete printing and machine learning. In this project, a groundbreaking initiative in Pakistan is presented which is the Development of Indigenous Concrete Printer and Mix Design, which represents a pioneering effort to revolutionize the construction sector in the country. The project's primary objective is twofold: first, the design and fabrication of an Indigenous Concrete Printer capable of constructing intricate concrete structures with unmatched precision; second, the implementation of machine learning algorithms, including Gaussian Process regression (GPR), Support Vector Machines (SVM), Decision Tree Regression (DTR), and XGBoost, to optimize the concrete mix design process.

The Indigenous Concrete Printer is a state-of-the-art construction technology specifically tailored to suit the unique requirements and challenges of Pakistan's construction industry. The printer’s boasts cutting-edge hardware and software, allowing for seamless integration and communication during the printing process. Its adaptability enables the creation of diverse architectural designs, empowering architects, and engineers to push the boundaries of creativity and design flexibility. The mix design optimization through machine learning algorithms is a groundbreaking addition to the project. By leveraging extensive datasets and predictive models, this technology revolutionizes the conventional concrete mix design approach, which often leads to material waste and increased costs. With the aid of machine learning, our system predicts the optimal mix proportions for specific structural demands, significantly enhancing resource efficiency and sustainability.

An essential aspect of this project is its uniqueness in Pakistan. The combination of an Indigenous Concrete Printer and machine learning-based mix design constitutes the first-of-its-kind initiative in the country. By introducing and integrating these advanced technologies, the project aimed to boost Pakistan's construction industry's productivity, economic growth, and environmental sustainability. In conclusion, the Development of Indigenous Concrete Printer and Mix Design is a pioneering project that promises to reshape the future of construction practices in Pakistan. This project aims to revolutionize the construction

landscape by offering unparalleled construction efficiency, design freedom, and resource optimization by the fusion of an Indigenous Concrete Printer and machine learning algorithms. As a trailblazing effort, it lays the foundation for a more sustainable, technologically advanced, and progressive construction industry in Pakistan, setting an inspiring example for other aspiring innovators and industries across the nation.

Chapter 1: Introduction

Chapter 1 covers introduction of the research topic and discusses the need behind this research and its objectives.

1.1. Introduction

There are several limitations to traditional construction technologies, including lengthy procedures, large material waste, restricted design flexibility, reliance on physical labor, and expensive costs (Kamali & Hewage, 2017). These drawbacks cause delays, higher costs, safety risks, environmental issues, and unaffordable housing options. By providing quicker, more cost-effective, and labor efficient alternatives, adopting cutting-edge construction techniques like 3D printing can get beyond these constraints and help create sustainable and affordable housing options (De Schutter et al., 2018). The development of 3D printing technology in recent years has made it an appealing option for resolving problems in the building sector. The fundamental idea behind 3D printing is additive manufacturing, which has many benefits over conventional construction techniques (Chong et al., 2018; Dilawar Riaz et al., 2023). It makes it possible to customize, create complicated geometries, and use less material waste, potentially revolutionizing the construction industry (Butkutė & Vaitkevičius, 2023).

By employing specialized printers to deposit layers of material, usually concrete, to produce building components, 3D printing in construction can generate complex architectural elements (C. Zhang et al., 2021). Numerous successful 3D-printed housing projects have shown the viability and promise of this ground-breaking method, which has gained popularity across the globe (*3D Printing of Houses Mexico*, n.d.; Goldin, 2014; Karyne Levy, 2014). These initiatives have demonstrated how 3D printing technology can considerably cut down on labor hours, material waste, and building costs while enhancing structural performance and design flexibility (Kim, 2013; Panda,

Tay, et al., 2018a). This thesis explores the creation of a domestic 3D concrete printer employing the idea of additive manufacturing technology to close the housing industry gap. The objective is to provide a low-cost and effective solution for repetitive construction in Pakistan using locally accessible materials and printing process optimization. This study addresses the critical need for creative methods for housing provision in line with the government's objective for affordable housing and sustainable development. To achieve these objectives, this thesis will draw upon the existing body of knowledge on additive manufacturing in construction, 3D printing materials and techniques, and global best practices in 3D-printed housing projects. It will employ a comprehensive research methodology to design, develop, and evaluate the performance and feasibility of the indigenous 3D concrete printer in the Pakistani context.

1.2. Problem Statement

"The introduction of this innovative technique in Pakistan is the need of the hour, considering the growing housing demand and reduced affordability of common citizens."

Pakistan, a populous country in South Asia, is dealing with serious issues in the housing industry(Jabeen et al., 2015). The demand for affordable housing has reached critical levels due to a growing population, increased urbanization, and limited resources (Altaf et al., 1993; A. Hasan & Arif, 2018). The dearth of housing and concerns with affordability are anticipated to worsen as Pakistan's urban population doubles by 2050, according to the UN(*UN-Habitat - A Better Urban Future | UN-Habitat*, n.d.). Among regional countries, Pakistan has the highest ratio of slums as a percentage of the total urban population as shown in the Figure 1.3. In Karachi and Hyderabad alone, there are around 1,300 slums, as per UNICEF (Babar et al., 2021). One of which is the settlements of Orange Town where, as of 2016, 2.4 million people lived, more than the population of Paris. Pakistan's traditional construction practices frequently rely on manual labor and

conventional methods, which leads to expensive prices and protracted construction times. These restrictions make it difficult to timely and economically supply appropriate homes for the populace. As a result, a sizeable segment of the population, especially those in low-income groups, struggle to find safe and reasonably priced homes.

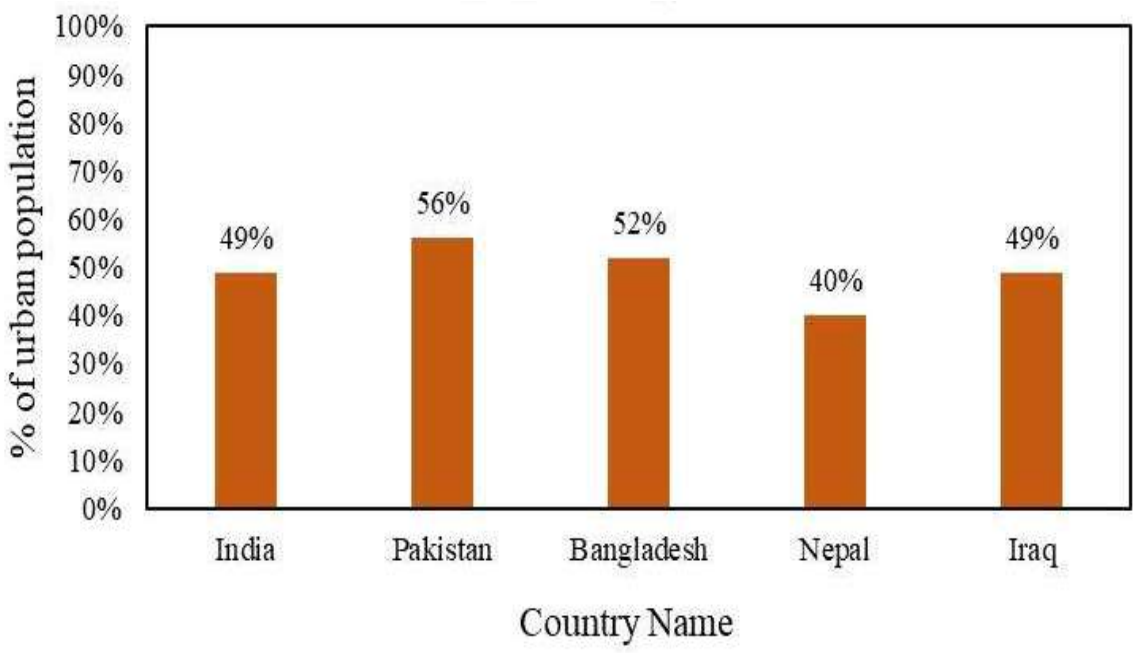

Figure 1.1: Dawn news report about increasing slums in Pakistan.

One of the major challenges common citizens' faces in Pakistan is reduced housing affordability. Rising construction costs, inflation, and limited purchasing power make it increasingly difficult for individuals and families to access decent and affordable housing options (Altaf et al., 1993). Further, Traditional construction methods in Pakistan contribute to the affordability problem. These methods are often labor-intensive and time-consuming, resulting in increased costs. Manual labor, which forms a significant part of traditional construction processes, drives up the expenses associated with wages, training, and safety regulations (A. Rehman & Jamil, 2021).

Innovative building methods, including 3D printing, have a lot of potential for tackling Pakistan's housing shortage and pricing issues. Construction time and labor requirements can be considerably

decreased by using 3D printing technology to produce building components quickly and efficiently using automated processes (Kim, 2013). Additionally, using 3D printers reduces material waste and enables precise customization, which lowers costs and increases design flexibility (Panda, Tay, et al., 2018b).

The introduction of 3D printing technology in Pakistan has the potential to revolutionize the building sector and address the housing issue. Innovative and effective construction solutions are desperately needed given the nation's fast urbanization, limited resources, and expanding population (Balletti et al., 2017). Pakistan may overcome the drawbacks of conventional construction techniques and give its inhabitants access to inexpensive home alternatives by utilizing 3D printing technology.

The printable concrete needs to have the following properties:

1.3. Project Objectives

The project objectives are:

- To develop a scalable prototype by developing frame, extruder, and movement system.
- To develop a printable mix design and assess its rheological and mechanical strength.
- To print various elements.

Chapter 2: Literature Review

Chapter 2 covers a detailed literature review of this technology and discusses the various mix design parameters for printable concrete mix design.

2.1. Background

The intersection of additive manufacturing with construction has paved the way for the rise of digital construction, and 3D concrete printing stands at the forefront of this technological revolution (Cho et al., 2019; Sahin & Mardani, 2022a). Due to its potential to completely transform conventional building techniques, additive manufacturing, often known as 3D printing, has drawn a lot of interest from the construction sector (Salet & Wolfs, 2016). The use of specialized printers to produce structural components is one of many additive manufacturing in building applications that researchers and practitioners have looked at(De Schutter et al., 2018; J. Zhang, Wang, Dong, et al., 2019). Studies have proven that 3D printing offers design flexibility and customization possibilities while reducing building time, labor expenses, and material waste (Bhattacherjee et al., 2021; J. Zhang, Wang, Dong, et al., 2019).

(a) (b) (c)

Figure 2.1: (a) Robotic Arm Printer (b) Gantry Based Printer*)* and (c) 3D Concrete Printed House (Uppala & Tadikamalla, 2017).

Recent data of UN Habitat suggests that over 1 billion people are living in slums and modular 3D printed concrete as a solution for the housing shortage across globe (*UN-Habitat - A Better Urban Future | UN-Habitat*, n.d.). UN-Habitat engages in policy development and advocacy to support the implementation of innovative housing solutions.

This technology offers a significant boost in efficiency, with increased construction speed and reduced formwork and labor costs accounting for **40-50%** of the construction expenses (Van Den Bergh et al., n.d.). Different types of concrete printer exist like Robotic arm and gantry based with their own gantry have their own advantages and disadvantages (Puzatova et al., 2022). The most efficient among these is gantry based (Uppala & Tadikamalla, 2017).

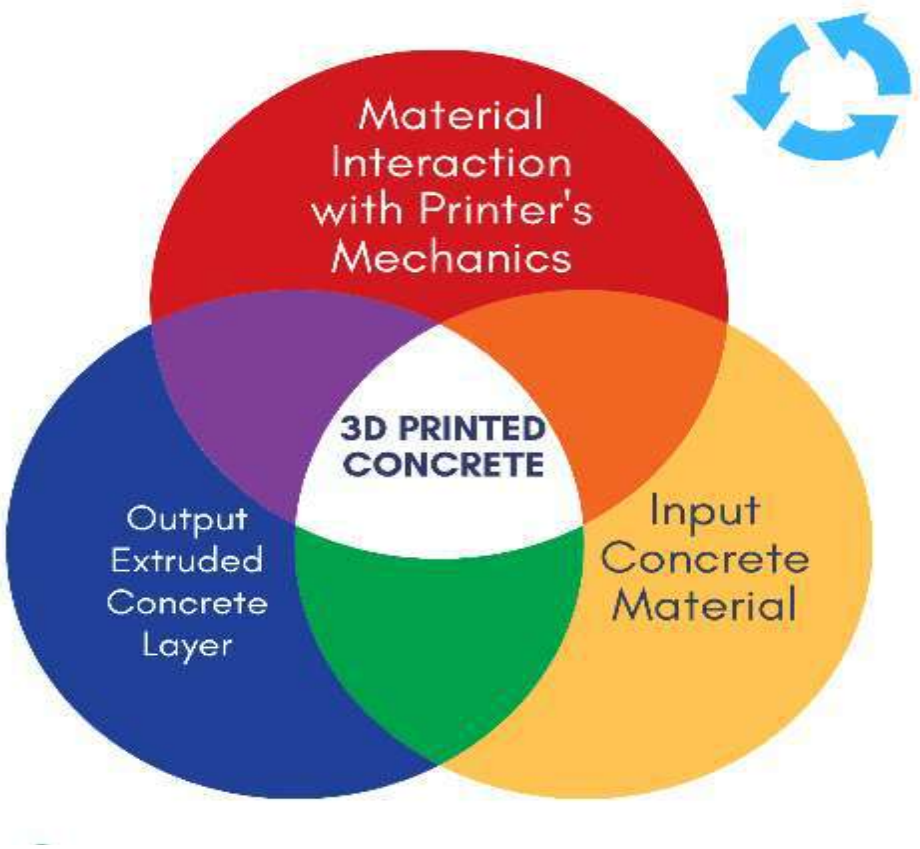

Figure 2.2: Complexity of 3D printed concrete mix design.

The concept of concrete printing is the same as normal 3D printing. An STL file which contains G-Code is generated via slicer and is used as an input by the 3D printer (Ngo et al., 2018). The choice of materials and printing techniques plays a crucial role in the success of 3D printed construction (C. Zhang et al., 2021). Concrete-based formulations have been widely used due to their availability, structural performance, and compatibility with additive manufacturing processes (Gjørv, 2008; Panda et al., 2018; Yao et al., 2017).

The most challenging aspect of 3D concrete printed mix is its interdependency of various parameters. A slight change in one property may induce a change in one or more other properties. Rheological properties like buildability, extrudability, and printability are interrelated, challenging and deceptive (Rahul et al., 2022). The key is to find an exquisite balance among all of them.

Investigating the application found in the literature, it can be seen that 50 houses were printed in 24 hours in Mexico, and importantly they sustained an earthquake of 7.4 magnitudes (*3D Printing of Houses Mexico*, n.d.). Largest concrete printed bridge in China (Goldin, 2014). Several successful 3D-printed housing projects worldwide have demonstrated the potential of this technology in addressing housing challenges. Notable examples include the *Apis Cor* project in Russia (Grigoriev & Martinov, 2018) and the *TECLA* project in Italy (Grigoriev & Martinov, 2018; Rollakanti & Prasad, 2022).

The complexity of the mix design of 3D-printed concrete lies in the interdependency of its mix design parameters: Buildability(Muthukrishnan et al., 2021a), extrudability (Nerella, Näther, et al., 2019), interlayer bonding (Marchment & Sanjayan, 2019), pumpability(Secrieru et al., 2017), anisotropy, and thixotropy (Barnes, 1997) and their subsequent sub-parameters. Printable concrete needs to have the following properties.

2.2. Mix Design Properties

2.2.1. Extrudability

The inherent ability of 3D printable concrete to flow smoothly from the extrusion intake chamber to the nozzle through a hose is one of its crucial rheological properties (Nerella, Näther, et al., 2019). Achieving optimal extrudability poses a challenge in the mix design since it requires minimizing dynamic shear stresses during extrusion (Jayathilakage et al., 2020). Different extrusion setups have specific criteria for determining extrudability. For contour crafting, it pertains to the concrete mix's ability to be extruded with minimal energy consumption, while for the piston-based mechanism, it concerns the energy required to push the concrete out of the nozzle in the desired shape(Cao et al., 2022; L. Yang et al., 2023). According to Nerella et al. a mix with

higher static and lower dynamic yield stress will exhibit greater extrudability (H. Chen et al., 2023).

Nevertheless, defining extrudability solely based on the power consumption of the extruder is not ideal. Qualitative characterization of printed concrete considers multiple parameters such as Printability, Layer adhesion, Surface finish, Workability, Rheological properties, setting time, Compressive strength, Durability, Material compatibility, and Fiber reinforcement, among others (Kaliyavaradhan et al., 2022). Chen et al. argue that extrudability should also consider print quality and filament continuity, broadening its scope as a property (M. Chen et al., 2018).

Linking extrudability to shape stability, continuous concrete flow, good surface finish, proper edges, and sufficient strength in complex printing processes through nozzle mechanics makes it a non-intrinsic and challenging property to achieve (Buswell et al., 2018). Various researchers have attempted to quantify the extrudability of concrete printing in different ways. For instance, Mag et al. defined extrudability using the Extrudability Constant (P_E) formula, which relates Spread Diameter, Rest Time, Max Spread, and Minimum Rest Time (Magnel & Zollman, 1954). A higher PE value indicates better extrudability and flowability, allowing for smoother and continuous printing. Conversely, a lower P_E value suggests lower flowability and may lead to difficulties during the printing process (Chu et al., 2023).Yang et al. quantified concrete extrusion from the nozzle based on the nozzle's traveling speed, finding that the optimum speed is two to three times the volumetric flow rate (H. Yang & Che, 2022). Andrew et al. proposed assessing extrudability by measuring the intensity of surface defects in the printed concrete object (Andrew Ting et al., 2022; J. Liu & Tran, 2022). A higher intensity of surface defects indicates lower extrudability and potential issues with the extrusion process and final product quality (Almazrouei et al., 2019).

Given the dependence of extrudability on various parameters, there is currently a need for globally

accepted standards to assess and define the extrudability of a concrete mix.

2.2.2. Buildability

Buildability refers to the ability of a deposited material to maintain its shape when subjected to subsequent loads, and it is particularly essential for formwork-free construction methods like 3D concrete printing (Muthukrishnan et al., 2021b). The complexity of buildability arises from the interplay of individual material properties and various building parameters, including geometric configuration and extrusion rate. Several factors influence buildability, such as the pattern of the element being printed and specific printing parameters like nozzle speed, height, and extrusion angular velocity (Joh et al., 2020a). Defective buildability of printed filaments can arise due to plastic collapse, elastic buckling, or a combination of both. Plastic collapse is governed by the yield strength of fresh concrete, while the stiffness of concrete controls elastic buckling. The Buildability Parameter (P_B) is an indicator that compares the concrete's relative stiffness penetration resistance to its slump height (M., 2016). A higher P_B value signifies that the concrete possesses greater stiffness penetration resistance than its workability, suggesting it is stronger and more resistant to deformation. Conversely, a lower P_B value indicates that the concrete has lower stiffness penetration resistance and higher workability.

The evaluation of the buildability of a fresh concrete mix can be done through penetration resistance (Tay et al., 2019a). The plastic failure criterion involves the compressive strength being twice the shear strength, which can be represented by the empirical equation(Rasheed et al., 2018):

$$\tau_p = mg / (2\pi rh + 2\pi r^2) \qquad 2.1$$

Here, τ_p represents the shear strength of concrete, h is the penetration depth of the Vicat needle, m is the mass of the Vicat needle, and r is the radius of the Vicat needle. Higher shear strength indicates greater resistance to shearing forces, making the printed concrete more robust and less

prone to deformation or failure under shear stresses.

Chen et al. characterized buildability using the "Shape Retention Factor" (M. Chen et al., 2018). A higher shape retention factor indicates that printed structures are more likely to maintain their shape and structural integrity during and after printing, indicating better buildability. Conversely, a lower shape retention factor implies a higher likelihood of deformation or loss of integrity during and after the printing process. In summary, buildability is a critical property for successful 3D concrete printing, ensuring that the deposited material retains its shape and structural integrity throughout the process. Achieving optimal buildability requires careful consideration of the concrete mixture's properties, printing parameters, and the geometric configuration of the structure.

2.2.3. Printability

Printability is a fundamental and intricate aspect of 3D concrete printing, encompassing a multitude of factors that directly influence the successful deposition and formation of concrete structures (Srinivas et al., 2022a). Beyond the conventional notion of printability, where ink adheres to paper, 3D printing in the realm of construction requires a delicate balance of properties to achieve desired outcomes. These properties include Pumpability, which ensures the smooth and consistent flow of the concrete mixture (Srinivas et al., 2022a) from the extrusion intake chamber to the printing nozzle, Extrudability, which focuses on the material's ability to be extruded with minimal shear stresses during the process (Faes et al., 2015; Wolfs & Suiker, 2019), and Buildability, which is crucial for retaining the structural integrity of the deposited material under subsequent loads and supporting the overall stability of the printed structure. To attain optimal printability in 3D concrete printing, special attention must be given to the rheological characteristics of the concrete mix (Roussel, 2018). The mixture needs to exhibit a delicate equilibrium between fluidity

and stability during the printing process. It should be sufficiently fluid to facilitate continuous extrusion and layer-by-layer formation, while also possessing a controlled setting time that allows for adequate bonding between layers and ensures proper consolidation(Jeong et al., 2019). Achieving this balance is a complex challenge, as it requires precise control over the concrete's flow properties, viscosity, and curing behaviour (Y. Zhang et al., 2019).

Researchers and engineers have developed various tests and models to assess and characterize the printability of concrete. These evaluations often involve analysing the yield stress, viscosity, and shear rate of the concrete under specific printing conditions. By understanding the intricate interplay of these rheological parameters, concrete mix designs can be optimized to enhance printability, enabling the construction industry to unlock the full potential of 3D concrete printing for innovative, efficient, and sustainable building practices. Embracing the advancements in printability will not only revolutionize the construction process but also open new avenues for architectural design, structural complexity, and material efficiency in the world of modern construction.

2.2.4. Anisotropy

Anisotropy in printed concrete refers to the directional dependence of mechanical and physical properties within the material, arising from the layer-by-layer deposition process used in 3D concrete printing (J. Chen et al., 2022). Unlike conventional concrete, which typically exhibits isotropic properties, where the material behaves uniformly in all directions, printed concrete may display variations in performance and behaviours depending on the orientation of its layers (Panda et al., 2017).

The anisotropic nature of printed concrete stems from the unique manufacturing process. Each layer is individually deposited, and the inter-layer bonding between successive layers might differ

from that of conventional cast concrete (G. Ma et al., 2019). As a result, the strength, stiffness, and other mechanical properties of the printed structure may vary depending on the orientation relative to the printing direction (Heras Murcia et al., 2020).For instance, the tensile strength and crack resistance of printed concrete may be weaker parallel to the printing direction, where the bonding between layers might not be as strong as in the perpendicular direction (Zhao et al., 2021). This anisotropic behaviour can impact the structural integrity and overall performance of the printed components, especially in load-bearing applications. To address anisotropy in printed concrete, researchers and engineers explore various strategies, such as optimizing printing parameters, modifying material compositions, and adjusting post-processing methods (Jiang et al., 2022). By carefully considering the anisotropic behaviour during the design and construction phases, it is possible to harness the advantages of 3D concrete printing while ensuring the structural reliability and efficiency of printed elements in real-world applications. Embracing anisotropy as a design consideration allows for innovative and creative solutions in construction, paving the way for a new era of complex and functional concrete structures (Marijnissen & Van Der Zee, 2017).

2.2.5. Thixotropy

Thixotropy in 3D concrete printing is a fascinating and critical aspect of the material's rheological behaviours (Barnes, 1997). Thixotropy refers to a phenomenon in which the viscosity of a material changes in response to changes in shear rate (Møller et al., 2006). In the context of printable concrete, thixotropy plays a vital role in achieving optimal printability and buildability during the 3D printing process. When the concrete mixture is at rest, it exhibits a higher viscosity, but when subjected to shear stress during extrusion through the printing nozzle, its viscosity decreases (Assaad et al., 2003; Jiao et al., 2021; Khayat et al., 2002). This behaviour is a result of the alignment of the concrete particles in the flow direction, leading to reduced resistance to flow. The

thixotropic behaviour of printable concrete is crucial for maintaining the material's shape and consistency during the printing process (González-Taboada et al., 2018). It allows for smooth and continuous extrusion, ensuring that the layers of the printed structure adhere well and maintain their structural integrity. This property is particularly valuable in 3D concrete printing, where precise layering and deposition are essential for creating complex and functional structures. Moreover, thixotropy also impacts the buildability of printed concrete (Y. Zhang et al., 2019). As the concrete is extruded and subjected to shear stress, the hydration products within the material continue to grow and form bridges between cement grains. This process gradually increases the yield stress of the concrete, making it stiffer over time. This increase in yield stress improves the buildability of the material, enabling it to support the weight of the preceding layers and resist segregation or deformation (Nerella, Beigh, et al., 2019; Soltan & Li, 2018).

Understanding and controlling thixotropy in printable concrete is vital for optimizing the printing process. Engineers and researchers can manipulate the thixotropic behaviours by adjusting the concrete mix composition, temperature, and shear rate. By carefully managing thixotropy, they can enhance the material's flowability during printing, achieve better layer-to-layer bonding, and improve the mechanical strength of the printed structures. Thixotropy empowers the 3D concrete printing industry to produce consistent, reliable, and structurally sound constructions, revolutionizing the way we build and design in the modern era.

2.2.6. Interlayer Bonding

Interlayer bonding in concrete printing is a crucial factor that directly impacts the structural integrity and overall quality of 3D printed concrete structures (Sanjayan et al., 2018). It refers to the adhesion and cohesion between successive layers of printed concrete as they are deposited, and it plays a fundamental role in ensuring the stability and durability of the final printed product (Van

Der Putten et al., 2019). Achieving strong and reliable interlayer bonding is essential for constructing load-bearing and robust structures (G. Ma et al., 2020; Zareiyan & Khoshnevis, 2017). Poor bonding between layers can lead to weak points, delamination, and reduced mechanical properties, compromising the structural performance, and potentially leading to structural failures (Y.-C. Wu & Li, 2022). Therefore, engineers and researchers focus on understanding and optimizing interlayer bonding to enhance the overall performance of 3D printed concrete.

Several factors influence interlayer bonding, including the material composition, printing parameters, environmental conditions, and post-processing techniques. Proper selection of concrete mix design with appropriate aggregate grading and binder content can significantly impact the bond strength between layers (S. Yu et al., 2020). Furthermore, controlling the printing temperature, nozzle speed, and extrusion rate during the printing process can ensure better adhesion and minimize the risk of delamination (Lao et al., 2021; Xu et al., 2019). To enhance interlayer bonding, additional techniques can be employed, such as modifying the printing path to improve contact between layers and employing vibration or compaction during or after printing to consolidate the layers. Post-processing methods, such as curing and heat treatment, can also be applied to improve the bond strength between layers (Nguyen et al., 2021; Yao et al., 2017). In conclusion, achieving robust and durable interlayer bonding is of paramount importance in 3D concrete printing. By understanding the factors influencing interlayer bonding and implementing suitable strategies, engineers and researchers can ensure the successful construction of high-quality and reliable 3D printed concrete structures, opening new possibilities for innovative and sustainable construction practices.

Chapter 3: The Development of a Scalable Prototype

Chapter 3 deals with the concept used for the indigenization of this technology and the fabrication of individual components of a concrete printer.

Developing a scalable prototype involves the following sub objectives.

- The design and validation of the frame.
- The design and validation of the extruding mechanism.
- The movement control System.

3.1. Design and Validation of the Frame

During the literature review, only one article provided guidance for the design of the frame for the 3D concrete printing setup (Jo et al., 2020). It recommended using a gantry frame with 3-axis movement. Collaborating with SMME (School of Mechanical and Manufacturing Engineering), a decision was made to purchase a CNC machine with dimensions of 15cm x 15cm x 10cm (length x width x height) and attach a relatively small 8mm circular diameter nozzle for the evaluation of printing cementitious materials(McGee et al., 2020).

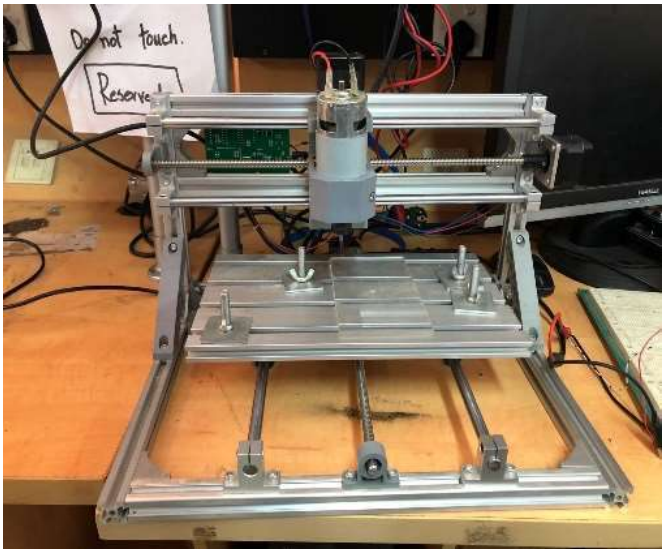

Figure 3.1 The CNC machine with bed size 15cm x 15cm x 10cm used for initial prototype design.

However, the initial prototype did not yield positive outcomes, and it became evident that a larger and more robust frame was necessary. The subsequent design iteration focused on fabricating a larger prototype comparable to conventional concrete cast specimens, such as beams or cubes. This would allow for meaningful comparisons between the printed and cast specimens following standard operating procedures, protocols, and guidelines. To visualize the end product and address the project objectives, a 3D model of the frame was generated.

After thorough research, it was clear that the gantry-based frame was sufficient for the additive manufacturing of concrete, providing the required 3-axis linear translational movement. Considering the need for cost-effectiveness and locally available materials, the decision was made to fabricate the frame using square iron pipes with cross-sectional dimensions of 3 x 3 inches and a gauge of 12. The final dimensions of the frame were determined to be 1.2 x 1.2 x 1 meter. To ensure the prototype's load-bearing capacity, welded connections were initially used for the frame's erection, as they offered the fastest and most convenient method. However, for future considerations and iterations, bolted connections would be preferred for ease of assembly and

potential adjustments or modifications.

In conclusion, the design process for the frame used in 3D concrete printing involved careful consideration of available literature, collaboration with stakeholders, and experimentation with prototypes to arrive at an optimal solution. The chosen gantry-based frame and locally sourced materials ensured a practical and cost-effective approach, while the 3D model visualization helped align the objectives of the project. The fabricated prototype, with its emphasis on load-bearing capacity and potential adaptability, laid the foundation for further advancements and refinements in the field of additive concrete manufacturing.

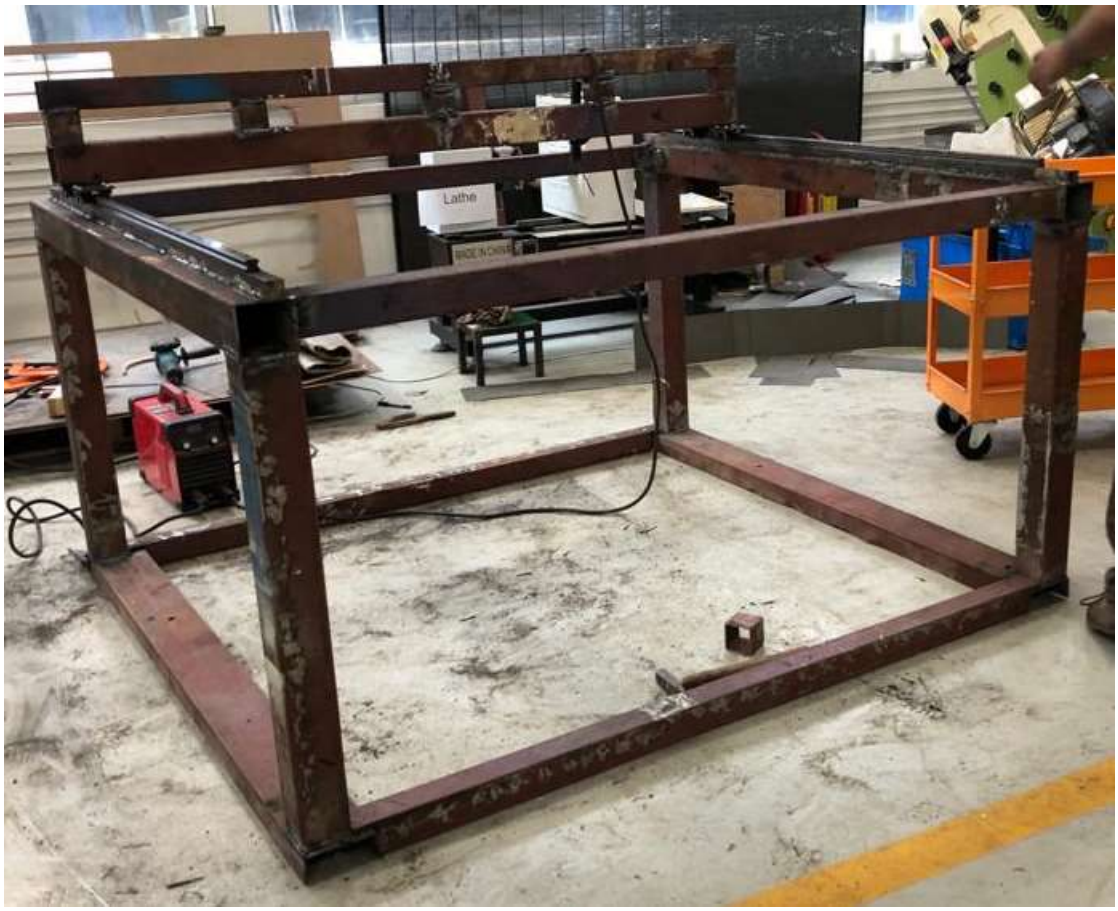

Figure 3.2 Fabrication of finalized prototype with dimensioning of 1m x 1m 0.5m.

3.2. The Design and Validation of the Extruding Mechanism

The design and validation of the extruding mechanism was the most critical aspect of our project as the whole success depended on its functional working(H. Chen et al., 2023). There are 2 types of extruding mechanisms that have been deployed into different types of concrete printers (Das et al., 2020) which are .Ram based extrusion mechanism, that employes ram to push concrete out through extruder in layers (Chong et al., 2018). Cavity based extrusion mechanism that moves the concrete material through pump in a sequence of small, fixed cavities along with the motion of motor accompanying a blade (Valkenaers et al., 2014). These extruders are shown in figure 3.3.

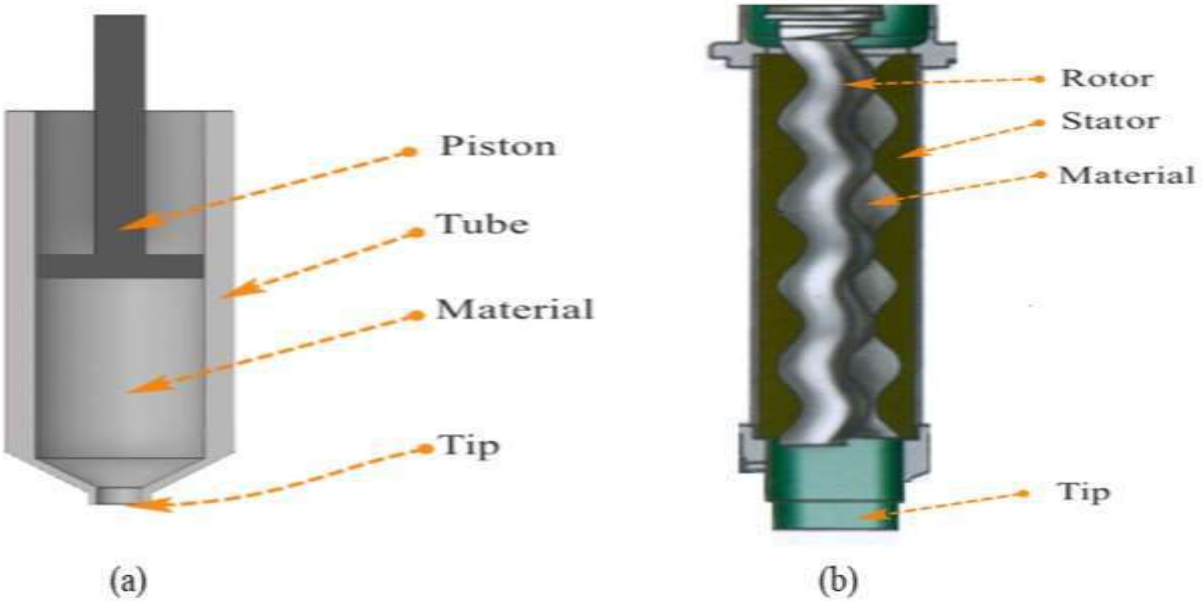

Figure 3.3 (a) Labelled diagram of ram-based extrusion mechanism. **(b)** Labelled Diagram of progressive cavity pump-based extruder. (Sanjayan et al., 2018).

Based upon intensive market research and literature review two extruding mechanisms were

shortlisted that could achieve our objectives which were Cavity based Extruding mechanism inform of progressive cavity pump and screw based extruding mechanism. Cavity based extrusion was very expensive and had to be imported so this option was excluded. It was found that a large screw was locally available as an auger blade used for boring holes in fields for agricultural purposes (Montepio, 2009). The auger blade was used to make an extruder by fabricating a shell around the blade which was comparable in size and had a very low tolerance. Auger blade extruding mechanism was deployed for being cheap, effective, indigenous, efficient having local abundance.

For the initial prototype an 8mm circular diameter extruder was fabricated but as it did not provide feasible results, so the auger blade extruder was used after careful consideration. A step-down shell container was designed and fabricated along with additional assemblies on the auger blade to ensure effective and uniform flow and extrusion of concrete. The additional assembly facilitated the downward pushing of concrete in the upper part of the shell by effectively minimizing the boundary layer effect. The maximum nozzle diameter was 3.5 inches in circular dimensions and the blade had a pitch/dia ratio of 0.96. For the extrusion multiple capacity motors were iteratively and continuously tested to find the desirable motor power that would ensure effective extrusion. The final head of the extruder is mountable giving the freedom of mounting any size or shaped nozzle to be mounted on it. The initial prototype had a motor of 60 W power and finalized larger prototype had a motor of 1.5 kW which as controlled using a VFD (Variable Frequency Drive) which allowed to control the speed of the auger blade in the extruder ranging from 0-60 rpm. The speed of the extruder blade can either be controlled manually using the PLC knob on the control panel or it can be controlled in the G-code either by giving a pre-defined value of rotational speed or by overriding the speed in the MACH 3 control panel. Due to budget constraints, the continuous

supply was not integrated. So, the extruder shell was made to carry a load of 35 kg of concrete material hence the frame was made of iron pipes having a higher thickness and use of welded connections.

3.3. Movement Control System

The movement profile of our concrete printing setup was a critical consideration, ranging from 6-axis (combining rotational and translational movements) to 3-axis (linear movement only). For our specific requirements, it was essential to have precise computerized numeric control (CNC) over 3-axis linear translational movement to ensure the necessary functional motion for successful concrete printing (Rahmatullah et al., 2021). It was discovered after conducting an extensive market survey and in-depth research that a CNC breakout circuit is shown in figure 3.4 was commonly utilized in locally available commercial CNC router setups (Jayachandraiah et al., 2014). This breakout board offered versatile motor control functionalities, making it a suitable choice for our application. To operate the CNC controller seamlessly, MACH3 software was opted, a widely used CNC operating software that proved compatible with our hardware and the CNC breakout board (Dwinugroho et al., 2019). MACH3 facilitated the precise control of our 3-axis linear translational movement, ensuring smooth and accurate motion during the concrete printing process (Boral, 2019).

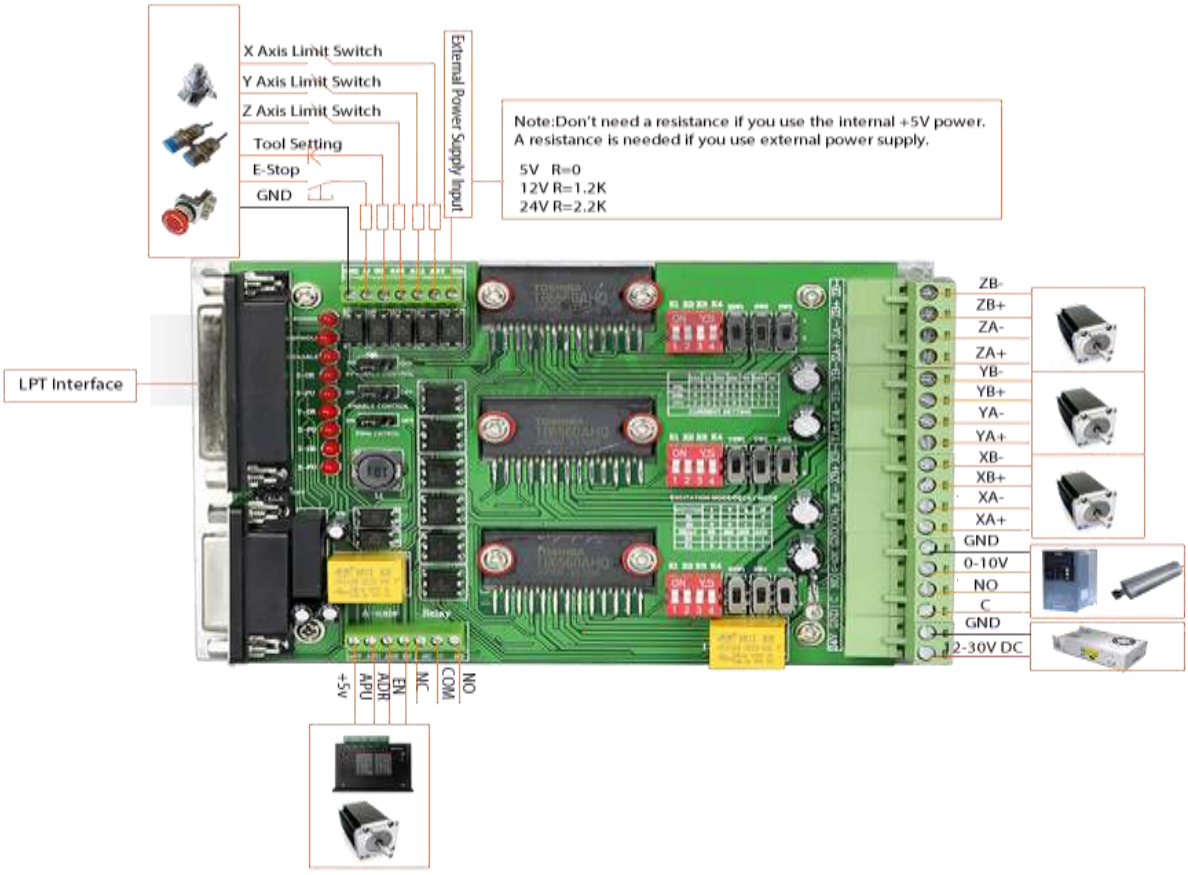

Figure 3.4 CNC Breakout board control circuit diagram.

This carefully selected CNC setup, with its focus on 3-axis linear translational movement and integration of MACH3 software, provided the necessary control and precision essential for successful concrete printing. By incorporating these advanced technological components into printing setup, the level of automation and efficiency required to produce complex and intricate concrete structures with high accuracy and reliability was achieved. This combination of hardware and software synergy empowered us to push the boundaries of 3D concrete printing, opening up new possibilities for innovative construction practices and architectural design. The control board has the specialty of operating and controlling both stepper and servo motors.

3.4. Stepper Motors

In the initial phase of our movement control system, stepper motors were due to several advantageous factors(Quatrano et al., 2017). Firstly, their cost-effectiveness made them a practical choice for project. Additionally, these motors were readily available in the local market, streamlining the procurement process. A stepper motor is shown in the figure 3.5. Another significant benefit was that they did not necessitate the use of additional controller driver circuits, simplifying the setup and reducing overall complexity (Madekar et al., 2016). Moreover, the low power consumption of stepper motors aligned with our goal of developing an energy-efficient concrete printing setup. The direct compatibility of these motors with the CNC breakout board further contributed to their ease of integration into our control system, streamlining the development process (Nae & Andrei, 2010).

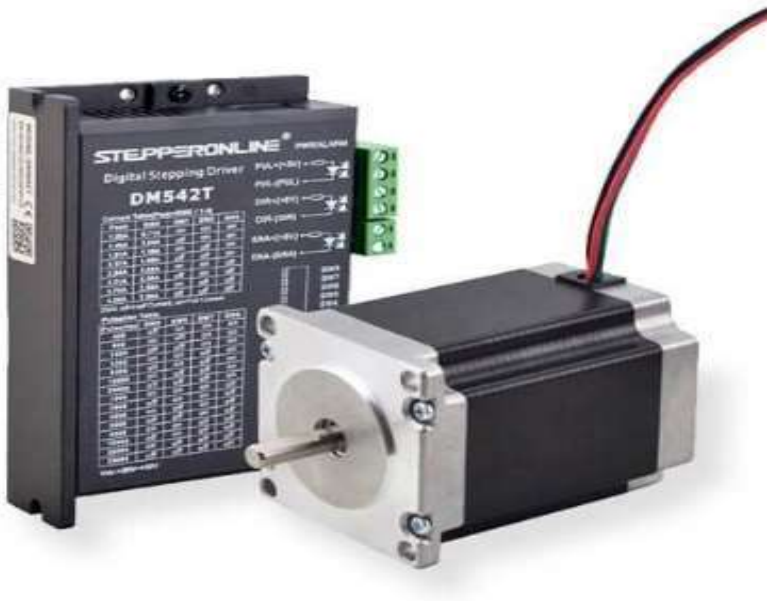

Figure 3.5 Typical Stepper Motor with control box (Madekar et al., 2016).

By employing stepper motors in the initial movement control, a practical, efficient, and straight forward approach was ensured to achieving the desired 3-axis linear translational movement required for our concrete printing setup. These cost-effective and locally available components,

coupled with their seamless integration with the CNC breakout board, played a significant role in laying the foundation for our successful concrete printing endeavours.

3.5. Servo motors

In pursuit of achieving consistent speed and improved performance, it was decided to opt transition from stepper motors to servo motors. This shift offered a myriad of advantages over using stepper motors, significantly enhancing our concrete printing setup. The motor is shown in the figure 3.6.

Figure 3.6: Typical Servo Motor with control box (Madekar et al., 2016).

One of the key benefits of servo motors was their ability to maintain consistent torque across the entire speed range(Patel, 2020). This ensured smooth and stable motion during the printing process, eliminating any potential fluctuations or jerky movements(Zheng et al., 2006). Another critical advantage of servo motors was their feedback loop control circuit. This feature allowed for precise and real-time monitoring of the motor's position, enabling accurate adjustments, and ensuring optimal performance (Mori et al., 2007). Servo motors also provided a larger working

envelope, allowing for a wider range of motion and versatility in the printing process. Their driver and encoder components facilitated precise positioning and control, enhancing the overall precision and accuracy of the concrete printing. Furthermore, servo motors boasted superior positioning accuracy and better resolution compared to stepper motors. This level of precision was vital for achieving intricate and complex designs with utmost detail and accuracy (M. M. Hasan et al., 2019a).

In addition to these technical benefits, servo motors offered noise reduction and smoother motion, resulting in a more refined and seamless printing experience (Kumar et al., 2017a). However, it is essential to note that the transition to servo motors did come with certain considerations. Unlike stepper motors, servo motors required an additional custom driver to accommodate the wiring for feedback loop sensors (B.-Y. Wu & Hsu, 2015). Consequently, this led to increased power consumption in comparison. Despite this drawback, the multitude of advantages provided by servo motors, including improved speed consistency, accuracy, and smoother motion, justified the switch and laid the groundwork for achieving exceptional results in our concrete printing endeavours.

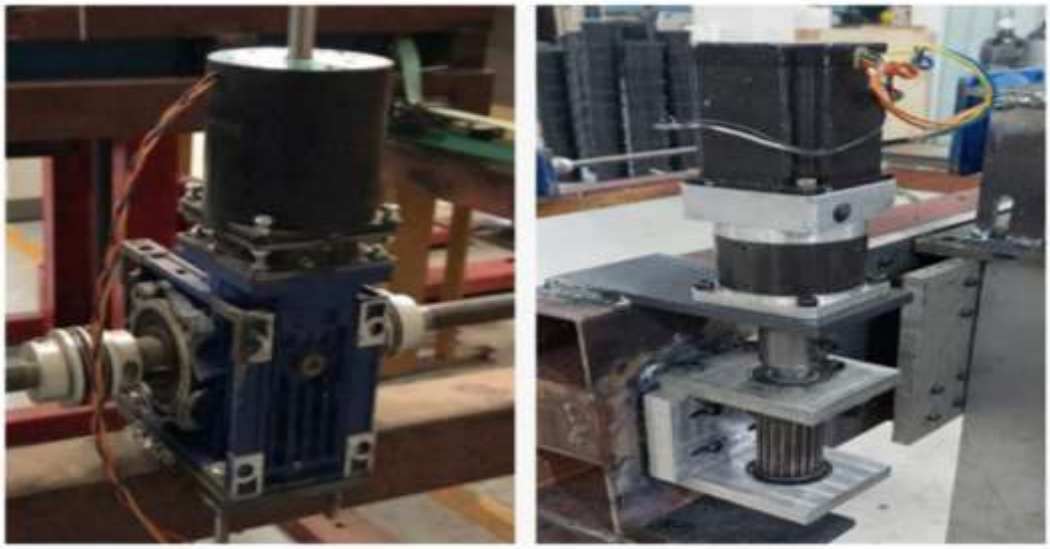

(a) (b)

Figure 3.7: (a) Servo motors assembly on the concrete printer which is used for axis movement. **(b)** Stepper motors assembly on the concrete printer used initially for axis movement.

During the initial stages of development, the precise speed of the linear translational movement was not immediately determined. Achieving synchronization required a rigorous trial and error process, involving continuous adjustments to the material properties until desired criteria and performance parameters were met. The finalized or idealized values for linear and extrusion speeds will be elaborated upon in subsequent chapters, following the development of a printable mix design. The integration of servo motors, particularly the incorporation of the feedback loop mechanism along with limit switches, significantly enhanced the performance and positioning accuracy of the system. While servo motors may have been more expensive than alternatives, their use was justified by the multitude of benefits and functionalities they provided. The implementation of limit switch sensors played a crucial role in controlling the end movement of the printer, ensuring precise and controlled positioning.

In conclusion, determining the optimal speed for linear translational movement was a dynamic process that necessitated continuous refinement of material properties. The use of servo motors, despite their cost, proved indispensable in achieving superior performance and accuracy in the concrete printing setup. The integration of feedback loop mechanisms and limit switch sensors further contributed to the overall success and reliability of the system, laying the foundation for a high-performing 3D concrete printing process.

3.6. Controlling Software

MACH 3 is a widely used and popular software known for its user-friendly interface, primarily utilized for operating computer-aided manufacturing tools, including routers, plasma cutters, CNC milling, and lathe machines. One of its key features is its support for the RS-274 programming

language, commonly referred to as G-CODE, which enables precise control over the movement and operation of the CNC machine (Kumar et al., 2017b). The interface is shown in the figure 3.8. In the MACH3 interface, the user inputs the G-CODE, which serves as a set of instructions for the CNC machine. The computer, acting as the intermediary, is connected to the CNC control circuit, which is responsible for regulating and directing the servo motors. This intricate connection between the software, computer, CNC control circuit, and servo motors ensures seamless coordination and accurate execution of the desired tasks.

The schematic depicts the straightforward and logical flow of commands from the user's input to the execution by the CNC machine. MACH3 acts as the control hub, facilitating smooth communication between the user and the CNC system, ultimately leading to precise and efficient operation of the manufacturing tools. In summary, MACH3's intuitive interface and support for G-CODE enable users to interact with CNC machines effortlessly. Through this software, they can input instructions that control the movement and functioning of the machine, allowing for the creation of intricate and intricate designs with exceptional accuracy and precision (M. M. Hasan et al., 2019b). The integration of servo motors and the CNC control circuit ensures that the executed tasks align with the user's intentions, making MACH3 an indispensable tool in the realm of computer-aided manufacturing (Sulaiman et al., 2020).

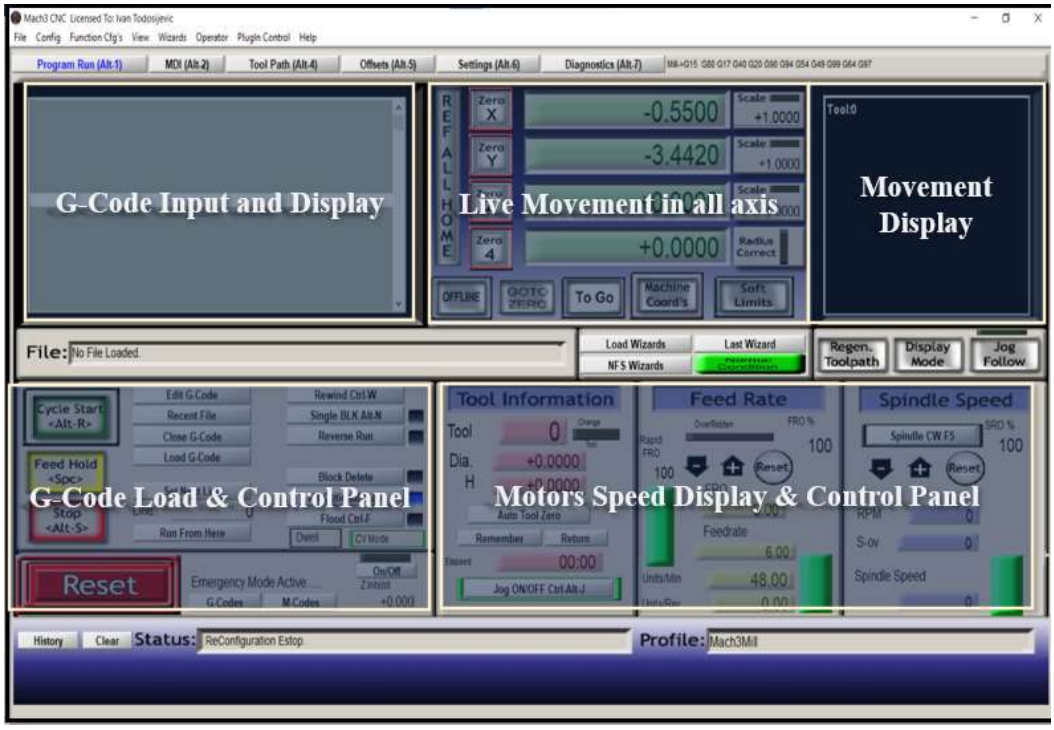

Figure 3.8: Interface of the Mach 3 Software used for concrete printer.

Also, MACH3 software offers extensive control over CNC machine operations, beyond G-CODE execution, with several key functionalities which can be integrated in the concrete printer.

1. G-Code Input and Display: Users can view and monitor the executed G-CODE instructions, facilitating real-time debugging and analysis.
2. Live Movement in all Axes: The interface displays live movement in three axes, showing speed and displacement counters in real time for accurate motion visualization.
3. 3D Movement Display: MACH3 provides a 3D visualization of head movement, enabling users to assess complex tool paths and designs with ease.
4. G-Code Load & Control Panel: Users can efficiently load and edit G-CODE instructions through the control panel, streamlining the CNC setup process.
5. Motors Speed Display & Control Panel: The software allows for precise control over motor speeds, enabling feed speed adjustments and sensor profile management.

With these functionalities, MACH3 empowers users to fine-tune movement profiles, monitor performance, and optimize CNC machine operations for enhanced precision and efficiency.

3.7. Discussion

The entire extrusion assembly was meticulously fabricated and assembled, employing a bolt-mounted aluminium plate to secure it onto the z-axis movement. This z-axis movement was expertly controlled by a ball screwdriver linear actuator. At the heart of the assembly, a powerful 1.5 kW motor was strategically positioned directly atop the extruder. This design consideration was carefully made to accommodate batch extrusion, as integrating a continuous supply for the concrete pump was not feasible at the time. To ensure structural strength and durability, high gauge MS Square iron pipes were utilized, providing robust support for the extrusion system.

With a maximum nozzle size of 3 inches and printable dimensions of 1 meter (length) x 1 meter (width) x 0.5 meter (height), the extruder's shell was skilfully designed to handle a substantial concrete material intake of approximately 60 kg in a single go. The step-down design of the shell played a vital role in facilitating double pumping of the concrete material. This ingenious approach involved a combination of gravity flow and the ram of the auger blade, ensuring a continuous and consistent flow of the printing material. The frame is shown in the figure below:

Figure 3.9: Fully fabricated concrete printer at first international housing expo'22 Islamabad.

The motor's connection to the auger blade was thoughtfully executed using a flexible shaft flange coupling. This coupling mechanism allowed for the smooth transfer of power from the motor to the auger blade, enabling efficient extrusion. Moreover, the connection was designed with modularity in mind, providing the flexibility to remove the auger blade easily for cleaning, maintenance, inspection, or in case of emergencies.

By incorporating these thoughtful design choices and engineering solutions, a robust, reliable, and adaptable extrusion assembly capable of meeting the demanding requirements of concrete printing was ensured. The modular design and consideration for batch extrusion exemplify the pragmatic approach taken to optimize the performance and versatility of the system. With the extrusion system in place. Now the target was the mix design formulation.

Chapter 4: Mix Design Formulation and Assessment

This chapter deals with the mix design formulation of printable concrete. It involves selecting a reference mix design and then iteratively changing the properties to obtain the printable mix design. Various tests that have been performed as also discussed below.

4.1. Base Mix Design

Given the absence of standardized guidelines for the mix design formulation of 3D printable concrete, our research took two approaches to address this challenge. The first approach involved starting from scratch and developing a mix design from fundamental principles (C. Zhang et al., 2021). However, considering the complexity and time constraints of this approach, it was decided to adopt a second approach. The second approach, inspired by the book "3D Concrete Printing Technology: Construction, and Building Applications"(Sanjayan & Nematollahi, 2019) by Dr. Behzad Nematollahi, involved selecting a base mix design from literature with printer properties comparable to our printer and iterating on it to make it suitable for printing with our specific printer. The base mix design selected is shown in Table 4.1.

This mix design, although lacking the inclusion of aggregates, served as a valuable starting point for our research (S. Yu et al., 2020). Recognizing the importance of incorporating aggregates in our mix design to enhance its mechanical properties and overall performance. Thus, objective was to optimize the mix constituents, including aggregates, to achieve printable and high-quality 3D printable concrete (Muthukrishnan et al., 2022). Exploring existing practices, it was discovered that many international companies treat their mix designs as intellectual property, making them unavailable for public reference.

Table 4.1: Reference mix design taken as start point for testing purposes.

Reference Mix		
Cement	9.1	Kg
Fly Ash (Class F)	3.9	Kg
Sand	4.22	Kg
Water	4.12	kg
Fiber	50	g
Fiber Percentage	0.30%	
S.P	13	g
W/B	0.317	
S/B	0.32	

Given this limitation, it was focused on selecting mix constituents that were locally and readily available in the market. By employing a systematic hit-and-trial approach, the iterative approach was used to optimize the mix design parameters, considering critical factors such as buildability, extrudability, thixotropy, anisotropy, and printability specific to our printing requirements (Kosmatka et al., 2002; A. U. Rehman & Kim, 2021). In total, 20 mix designs were developed and evaluated, systematically varying each parameter to explore its influence on the concrete's properties. This iterative process involved incrementally increasing or decreasing the proportions of individual constituents while closely monitoring the resulting changes in printability and performance.

4.2. Optimization of Mix Design

The optimization of the base mix design involved a systematic approach, where various factors such as workability, strength, and printability were considered. Initially, a series of trial-and-error iterations were performed. Different proportions of constituents, including cementitious materials, aggregates, and admixtures, were systematically varied in order to assess their impact on the desired properties. Each mix formulation was carefully evaluated for workability, strength development, and printability. However, due to limitations or the unavailability of suitable computational models specific to 3D printable concrete, the optimization process predominantly relied on empirical methods. Consideration of factors such as workability, strength, and printability: Throughout the mix design optimization, critical factors such as workability, strength, and printability were carefully considered (Papachristoforou et al., 2018). Workability played a crucial role in ensuring the concrete's flowability during the printing process, directly affecting the successful deposition of each layer and overall print quality. Strength was a fundamental parameter that determined the structural integrity and load-bearing capacity of the printed components (Gupta, 2007; Keating & Hannant, 1989; Panda et al., 2018). Printability encompassed various aspects, including extrudability, layer adhesion, dimensional accuracy, and the prevention of defects. To achieve an optimized mix design, adjustments were made to the proportions of binders, aggregates, and admixtures while considering these factors. The goal was to strike a balance between workability and strength by selecting suitable materials and adjusting their quantities. Printability was assessed through various qualitative and quantitative measures, and modifications were made to the mix design to improve the extrusion process, enhance layer adhesion, and ensure the successful printing of complex geometries (Sanjayan & Nematollahi, 2019).

In order to validate and determine the best-performing mix design, a series of rigorous tests were

conducted on each formulation. The purpose of these tests was to evaluate different aspects of the concrete's behaviour and characteristics, such as workability, strength, flowability, and dimensional stability. The test results were thoroughly examined, and the performance of each mix design was analyzed to find the ideal combination of constituents and their proportions that fulfilled the printing requirements. The entire mix design exploration, from the initial selection to subsequent optimization, allowed for the development of a customized and printable concrete mix tailored to the specific 3D printing application. Throughout the iterative process, both available references and local materials were taken into consideration to refine the mix design parameters and eventually identify the most suitable formulation for the research objectives.

4.2.1. Slump Test

The slump test is utilized to assess the flowability of concrete, providing valuable insights into its printability (Rahul & Santhanam, 2020; Srinivas et al., 2022b). Given the challenges in achieving consistent results for the fresh state properties of 3D printable concrete, efforts have been made to standardize the mixing procedure to ensure reliable and reproducible outcomes. In this study, a mixing procedure from the literature was adopted, which has proven effective for similar 3D printing applications.

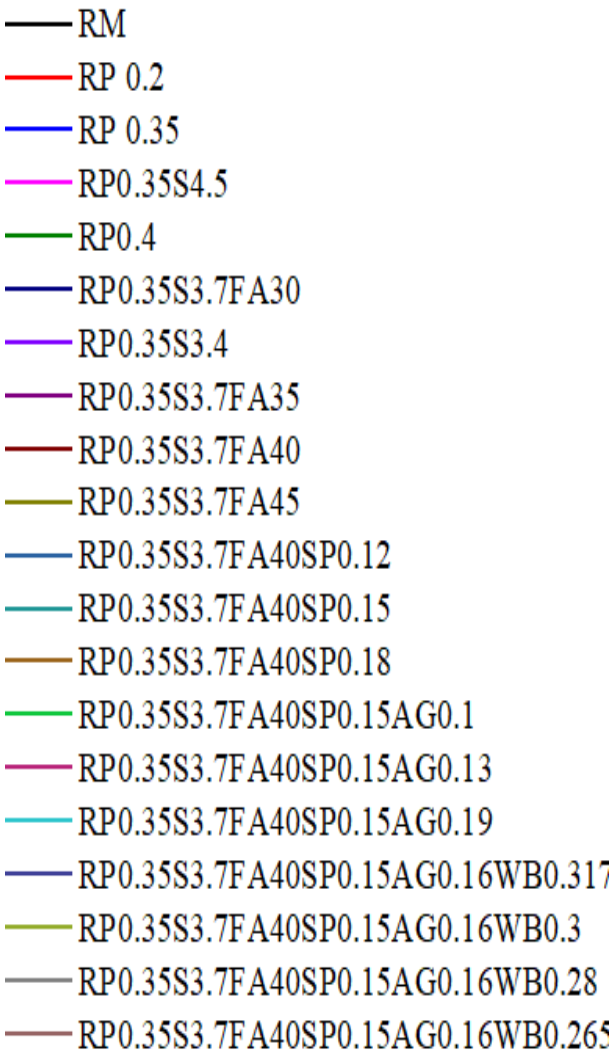

Figure 4.1: Nomenclature of mix designs subjected to slump cone testing.

To determine the maximum buildable slump and the minimum extrudable slump for the specific printer, slump tests were conducted on the 3D printable concrete mix. The nomenclature of mix designs used is shown in figure 4.1. To understand this nomenclature, the following table 4.2 can be referred to in terms of the base mix design.

Table 4.2: Reference mix adjustments.

Nomenclature	Reference Mix Adjustment (Units)
RM	Reference Mix Proportion
RP (6mm)	Addition of Polypropylene Fiber (%).
S (River Sand)	Sand Addition (kgs)
FA (Fly Ash Class F)	Fly Ash Addition (Replacement of cement)
SP (Polycarboxylate)	Super Plasticizer (%)
AG (Aggregate retained on sieve # 4, Passing ¼ inch)	Aggregate (aggregate/binder)
WB	Water to Binder Ratio

The buildable slump indicates the highest slump value at which the concrete can be successfully deposited and maintain its shape during printing(Tay et al., 2019a). Conversely, the extrudable slump refers to the lowest slump value that allows for sufficient extrusion through the printer nozzle (Tay et al., 2019b). Through extensive experimentation and analysis, the maximum buildable slump for the printer was identified to be 6.5 inches. Beyond this value, the buildability of the concrete significantly decreased, leading to poor structural integrity during printing. Similarly, the minimum extrudable slump was determined to be 2.5 inches. Below this value, the extrusion process became inadequate, hindering the successful deposition of the concrete. To optimize the mix design with respect to the slump value, the proportions of the mix constituents were carefully adjusted (Nadimalla et al., 2022).Slump test is shown in the figure 4.2.

Figure 4.2: Slump cone test to measure the slump of concrete.

It is crucial to note that the rheology of 3D printable concrete is time-dependent, underscoring the importance of quantifying and understanding its behaviour to achieve a balance between buildability and extrudability. By considering the regions of zero buildability and zero extrudability, a printability limit zone was established. Within this zone, five specific mix formulations were selected and separated from the total of 20 developed mixes, as mentioned previously (Chandra & Björnström, 2002). These selected mixes were deemed suitable for 3D printing based on their slump values and demonstrated a favorable balance between buildability and extrudability (H. Chen et al., 2023; M. Chen et al., 2020). The results and insights gained from the slump tests played a critical role in guiding the optimization of the mix design, enabling the identification of the range of slump values most suitable for the printer and 3D printing application.

4.2.2. Deformation Test

The deformation test was conducted to evaluate the stability of the printed structure and assess the

deformation behavior of the concrete mix design. The following description provides additional details about the test, its execution, and the relationship between deformation behavior and mix design parameters (K. Yu et al., 2021).

Figure 4.3: Deformation test under 500g loading.

The deformation test serves as a crucial measure to ensure that the printed concrete structure remains stable and maintains its desired shape. Although specific standards or testing protocols for 3D concrete printing are yet to be established, researchers have developed their own testing methodologies to address this need. To assess the buildability of the printed structure, a deformation test was conducted using a vacate apparatus mold. In this test, a loading of 500g was applied to the printed concrete sample, and the resulting deformation was measured shown in the figure 4.3. The maximum allowable deformation typically falls within the range of 10-15% according to the literature (M. Chen et al., 2020, 2021; Goldin, 2014; Jiao et al., 2021; Nerella, Beigh, et al., 2019; Soltan & Li, 2018). In our research, a similar approach was adopted to evaluate the deformation behavior of our mix design. However, to mimic the loading conditions experienced during subsequent layer depositions, a higher loading of 1000g was applied to the concrete layer.

This increased loading allowed for a more representative assessment of the deformation response. By performing the deformation test on the printed samples, deformation values were measured and compare them to the acceptable limits (Joh et al., 2020b; Muthukrishnan et al., 2021c). Mix designs that exhibited deformations within the defined limits were considered suitable for 3D printing, indicating their ability to maintain structural stability during the printing process. Conversely, mix designs that exhibited excessive deformation or deformation below the desired range were excluded from the selection. Through the deformation test, two additional mixes were eliminated from the previously selected five mixes out of the total of 20 developed mixes. One mix demonstrated the highest deformation, indicating poor stability and unsuitability for printing. Similarly, another mix exhibited the least deformation, suggesting potential issues related to its mechanical properties or workability. Analyzing the deformation behavior and its relationship to mix design parameters provided valuable insights into the printability and stability of the concrete structure. The results from the deformation test allowed us to further refine the selection of mix designs, ensuring that only those with favorable deformation characteristics were considered for subsequent evaluation and testing.

4.2.3. Optimization of Printing Speed

Optimizing the printing speed is another critical aspect of 3D concrete printing. It involves investigating the impact of printing speed on the quality of the printed structures and finding a balance between the extrusion speed and the linear speed of the printer in the x, y, and z directions. To ensure the structural integrity and dimensional accuracy of the printed structures, it is essential to find an optimal printing speed that allows for proper material deposition and layer formation (Gordon & Hillery, 2005; Zhao et al., 2022). If the linear speed of the printer is significantly higher than the extrusion speed, it can result in a tearing effect, compromising the structural integrity of

the printed components. On the other hand, if the extrusion speed is much higher than the linear speed, it can lead to zero buildability, preventing the successful deposition of the material.

In our research, the linear speed of the printer was kept constant and focused on finding the relationship between the extrusion speed and the aspect ratio of the printed layer. Various experiments were conducted with different mix designs to evaluate the influence of printing speed on the structural integrity and dimensional accuracy of the printed structures(Xu et al., 2019). The experimentation process involved systematically varying the printing speeds and observing the resulting quality of the printed components. By analyzing the relationship between extrusion speed and aspect ratio, the optimal printing speed range was identified for each mix design.

The experimental results were compiled and analyzed, leading to the development of a graph that visually represented the relationship between extrusion speed and aspect ratio for the different mix designs. This graph served as a valuable tool for understanding the interplay between printing speed and the desired quality of the printed structures (Lao et al., 2017).

The optimization of printing speed has implications for future research and development of mix designs for 3D printing. It highlights the need to carefully consider the balance between extrusion speed and linear speed to achieve optimal printability and structural integrity. Further research can focus on exploring advanced techniques or algorithms to automatically adjust the printing speed based on the specific mix design characteristics and desired printing outcomes.

Overall, the optimization of printing speed plays a significant role in achieving high-quality, dimensionally accurate, and structurally sound 3D-printed concrete structures (S. Ma et al., 2021). By fine-tuning the extrusion speed in relation to the linear speed, it becomes possible to achieve optimal printing performance and pave the way for further advancements in the field of 3D concrete printing (Khayat et al., 2014).

The aim was to find the optimal combination that would facilitate the smooth extrusion and printing process while maintaining the necessary structural integrity.

Fly ash, being a supplementary cementitious material, was added to the mix to enhance workability. The fine particles of fly ash acted as ball bearings, reducing friction between the cement grains and promoting better cohesion within the mixture. This resulted in increased flowability and reduced risk of segregation during printing.

Cement, being the primary binder in concrete, played a crucial role in determining workability. Higher cement content was expected to improve strength, but it was also found to increase the viscosity of the mix, making it less fluid. As a result, an appropriate cement-to-aggregate ratio was established to strike a balance between strength and workability.

Water content was a critical factor influencing workability. The right water-cement ratio was crucial in achieving the desired consistency without causing excessive bleeding or slump loss. A higher water content could lead to decreased viscosity, making the mix more fluid, but it also risked compromising the final strength.

Superplasticizer, an essential admixture, was used to enhance the workability of the concrete. By dispersing the cement particles and reducing the water demand, superplasticizer increased the fluidity of the mix. This significantly improved the ease of extrusion during 3D printing, allowing for complex shapes to be printed without compromising the structural integrity.

Accelerators were incorporated into the mix to promote early-age strength development and accelerate the setting time. This helped in achieving the desired workability within a shorter period, ensuring the concrete was ready for printing in a timely manner.

The selection of sand and aggregate sizes also had a notable impact on workability. Well-graded aggregates with suitable particle sizes were preferred, as they enhanced the packing density and

improved the flow behavior of the mixture. This resulted in a more workable concrete mix, which was crucial for the successful 3D printing process.

To understand the concrete's behavior over time, stress-strain curves were plotted while observing the slump values at different time intervals, up to 40 minutes. This detailed analysis allowed the researchers to identify the optimum slump value that would maintain the desired consistency of the concrete during the entire printing process.

In conclusion, the experiment's meticulous analysis and testing of various constituents in the concrete mix enabled the researchers to develop a well-balanced, workable concrete mixture tailored specifically for 3D printing applications. These findings were invaluable in optimizing the concrete mix design and ensuring successful 3D printing with the desired structural properties.

4.3. Results

4.3.1. Slump Test

The aim was to find the optimal combination that would facilitate the smooth extrusion and printing process while maintaining the necessary structural integrity. The corresponding results are shown in figure 4.4. The zero buildability and extrudability regions have already been discussed in 4.2.1. and are marked in the following figure.

The nomenclature for coded mix designs is shown in figure 4.1. Fly ash, being a supplementary cementitious material, was added to the mix to enhance workability. The fine particles of fly ash acted as ball bearings, reducing friction between the cement grains, and promoting better cohesion within the mixture. This resulted in increased flowability and reduced risk of segregation during printing. Cement, being the primary binder in concrete, played a crucial role in determining workability. Higher cement content was expected to improve strength, but it was also found to increase the viscosity of the mix, making it less fluid (J. Liu et al., 2022). As a result, an appropriate

cement-to-aggregate ratio was established to strike a balance between strength and workability (Aïtcin, 2000).

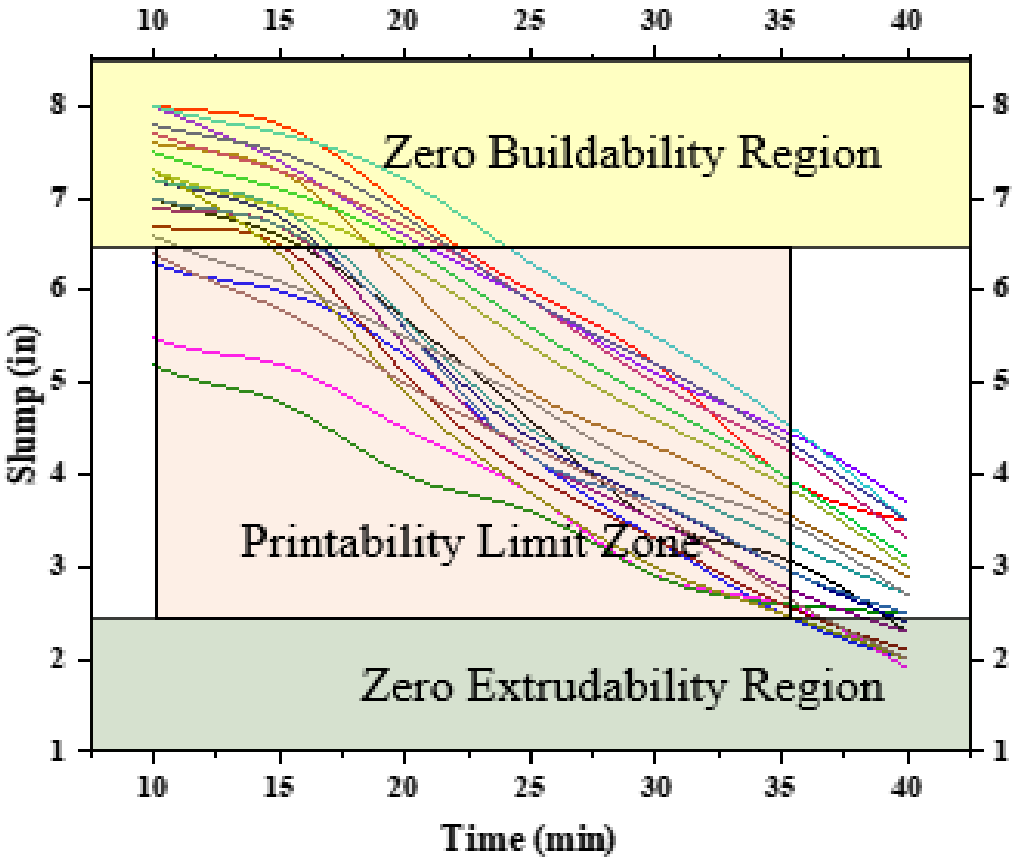

Figure 4.4: Results of the slump test performed up to 40 minutes for each mix.

Water content was a critical factor influencing workability. The right water-cement ratio was crucial in achieving the desired consistency without causing excessive bleeding or slump loss. A higher water content could lead to decreased viscosity, making the mix more fluid, but it also risked compromising the final strength. Superplasticizer, an essential admixture, was used to enhance the workability of the concrete. By dispersing the cement particles and reducing the water demand, superplasticizer increased the fluidity of the mix (Rasheed et al., 2018). This significantly improved the ease of extrusion during 3D printing, allowing for complex shapes to be printed

without compromising the structural integrity (Sanjayan & Nematollahi, 2019).

Accelerators were incorporated into the mix to promote early-age strength development and accelerate the setting time. This helped in achieving the desired workability within a shorter period, ensuring the concrete was ready for printing in a timely manner (Wongkornchaowalit & Lertchirakarn, 2011). The selection of sand and aggregate sizes also had a notable impact on workability (Bhattacherjee & Santhanam, 2020). Well-graded aggregates with suitable particle sizes were preferred, as they enhanced the packing density and improved the flow behaviour of the mixture. This resulted in a more workable concrete mix, which was crucial for the successful 3D printing process. To understand the concrete's behaviour over time, stress-strain curves were plotted while observing the slump values at different time intervals, up to 40 minutes. This detailed analysis allowed the researchers to identify the optimum slump value that would maintain the desired consistency of the concrete during the entire printing process. So, based upon the defined region mix the following mix were selected shown figure 4.5.

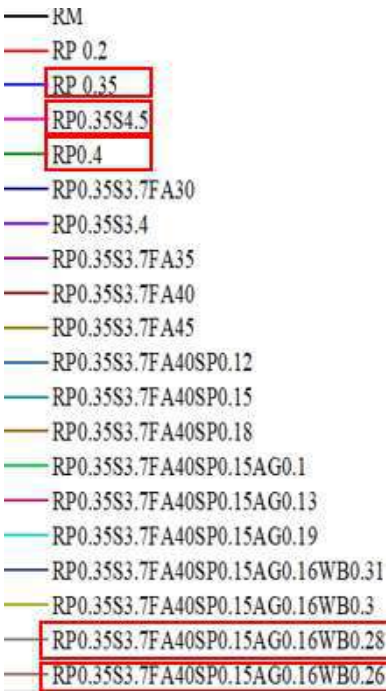

Figure 4.5: The marked mix designs based upon defined zones.

4.3.2. Deformation Test

The effect of various constituents on the workability of the concrete mixture was investigated using the Vicat mould sample under a loading of 500g. This experiment aimed to understand how the addition of fly ash, cement, water, superplasticizer, accelerator, sand, and aggregate influenced the flow behaviour of the concrete and its suitability for 3D printing. Fly ash, as a supplementary cementitious material, was added to the mix to improve workability under the specified loading conditions. Its fine particles acted as lubricants, reducing the friction between cement grains, and enhancing cohesion. This allowed the concrete to flow more freely in the Vicat mould, ensuring smooth and consistent results. Cement content was carefully adjusted to strike a balance between workability and strength under the 500g loading. Higher cement proportions could increase the mixture's viscosity, affecting its flowability, while lower amounts might compromise the final strength. An optimized cement-to-aggregate ratio was determined to achieve the desired workability while maintaining structural integrity. Water content was a critical factor in achieving the appropriate consistency for printing under the specified loading. The water-cement ratio was carefully controlled to prevent excessive bleeding or slump loss, ensuring the concrete remained workable during the Vicat test. Superplasticizer was used to enhance workability by reducing the water demand and increasing the fluidity of the mix. The addition of superplasticizer helped achieve better flow behaviour, allowing the concrete to maintain its shape under the 500g loading, which is crucial for successful 3D printing.

Accelerators were included in the mix to promote early-age strength development and accelerate the setting time under the specific loading conditions. This ensured that the concrete attained the desired workability within the designated timeframe, enabling efficient printing.

The selection of sand and aggregate sizes played a significant role in the workability of the concrete

sample under the 500g loading. Well-graded aggregates with appropriate particle sizes were chosen to enhance the packing density and improve flowability in the Vicat mould.

Stress-strain curves were plotted for the concrete sample under the specified loading, observing the slump values at different time intervals up to the designated testing period. This comprehensive analysis helped identify the optimal slump value, ensuring the concrete maintained the desired consistency for printing throughout the Vicat test. The results of the testing are shown in figure 4.6.

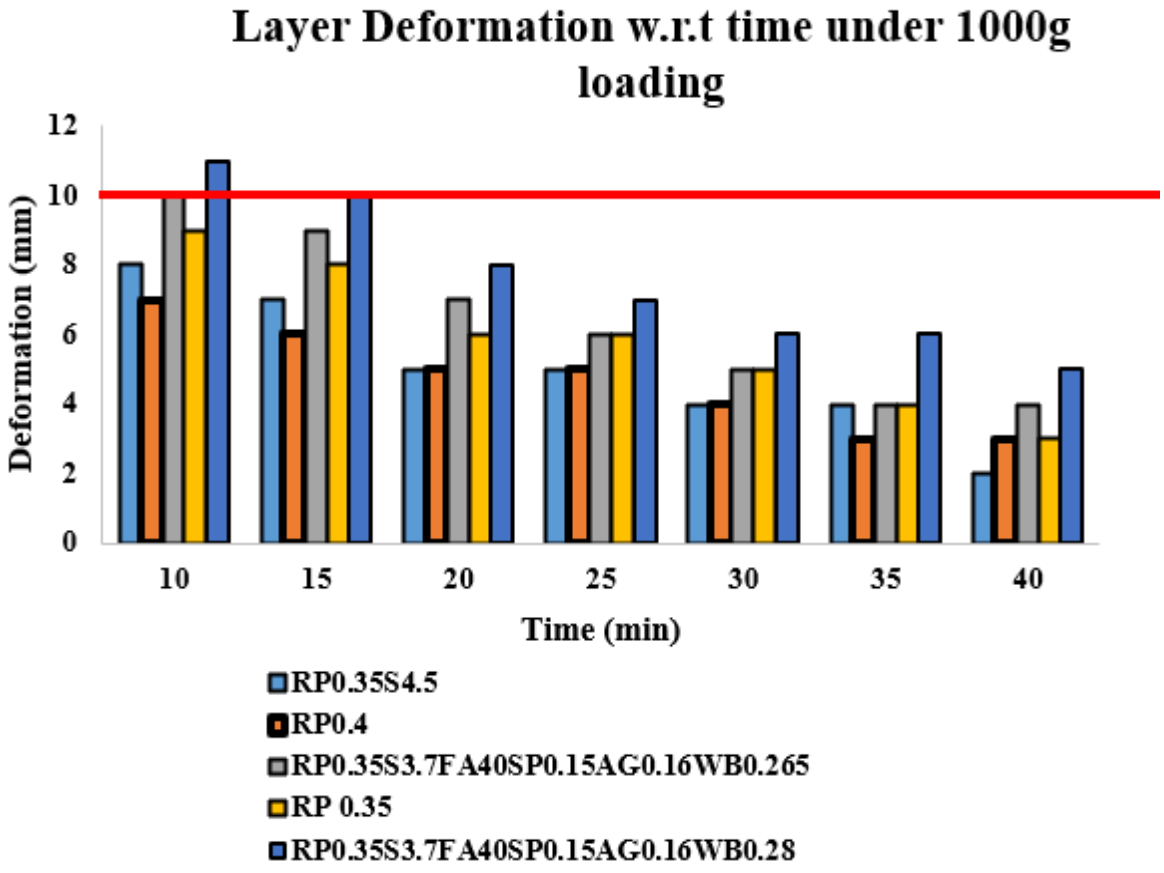

Figure 4.6: Layer vs deformation curve for different selected mix after slump cone test subjected to boundary conditions.

4.3.3. Optimization of Printing Speed

To enhance the packing density and improve flowability in the Vicat mould In the previous

discussion, the importance of optimizing the printing speed was explored for 3D concrete printing, specifically focusing on achieving a balance between linear and extrusion speed. The target linear speed is a crucial parameter in this optimization process, as it directly affects the printing quality and overall functionality of the printed structure. The challenge lies in finding the optimum speed that ensures functional printability while minimizing layer settlement during continuous extrusion. Yang et al. (Y. Zhang et al., 2019) highlighted the significance of selecting an appropriate printing speed for different concrete mixes and printing setups. Their research emphasized that the printing speed cannot be universally applied across all formulations due to variations in material properties and printing conditions. Instead, it should be tailored to suit each mix's specific characteristics and the unique demands of the printing setup. By maintaining the target linear speed, it is possible to achieve consistent extrusion and deposition of layers, resulting in a more uniform and stable structure. This mitigates the risk of layer settlement, ensuring that each layer adheres to the previous one seamlessly, and reduces the potential for deformations or weak points in the final printed object.

Furthermore, finding the optimum printing speed is critical to guaranteeing that the extruded material can be continuously deposited without interruptions or defects. A proper balance between linear and extrusion speed ensures a steady flow of the concrete mix, preventing clogging or irregularities in the printed layers. In our research the linear speed was fixed at 32mm/sec and extrusion speed was varied to find the optimum combination as shown in figure 4.7.

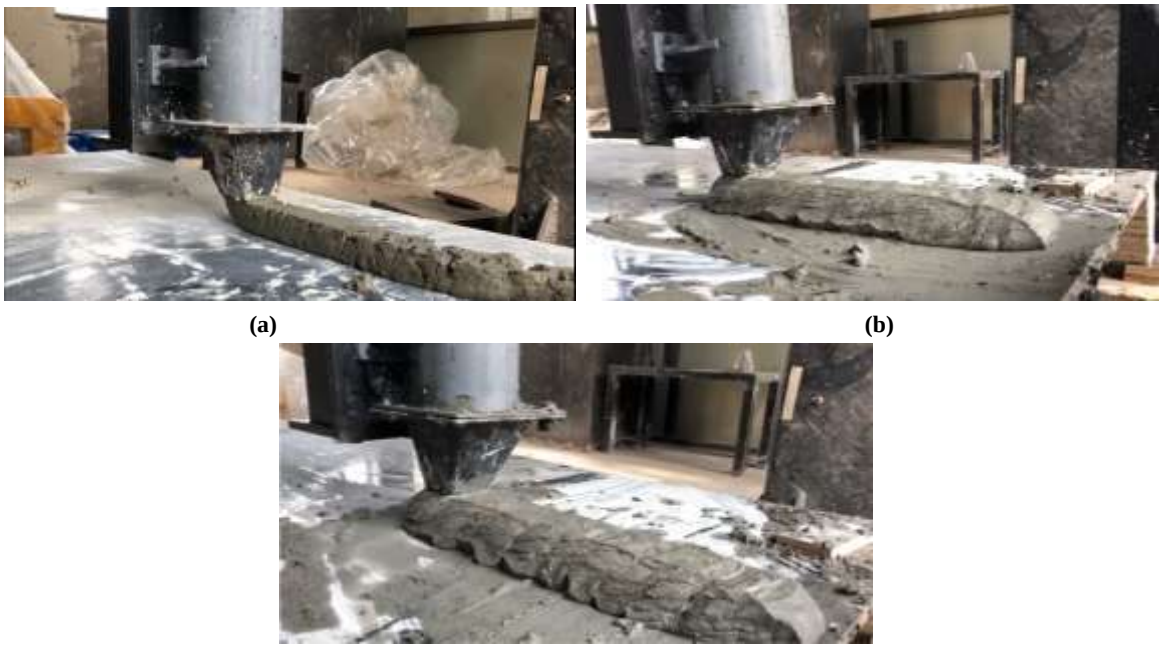

(a) **(b)**

(c)

Figure 4.7: Printing speed vs extrusion speed hit and trail testing at fixed linear speed of 32 mm/sec. (a) at 15 rpm, (b) 33 rpm and (c) 40 rpm

In conclusion, the discussion on printing speed optimization highlights the significance of striking the right balance between linear and extrusion speed. The target linear speed should be carefully determined to ensure functional printability and minimize layer settlement during continuous extrusion. As different concrete mixes and printing setups may exhibit varying behaviors, it is essential to customize printing speeds to achieve optimal results for each specific case. The results of this testing as shown in figure 4.8. Increased speed gives tearing effect and decreased speed gives overflow.

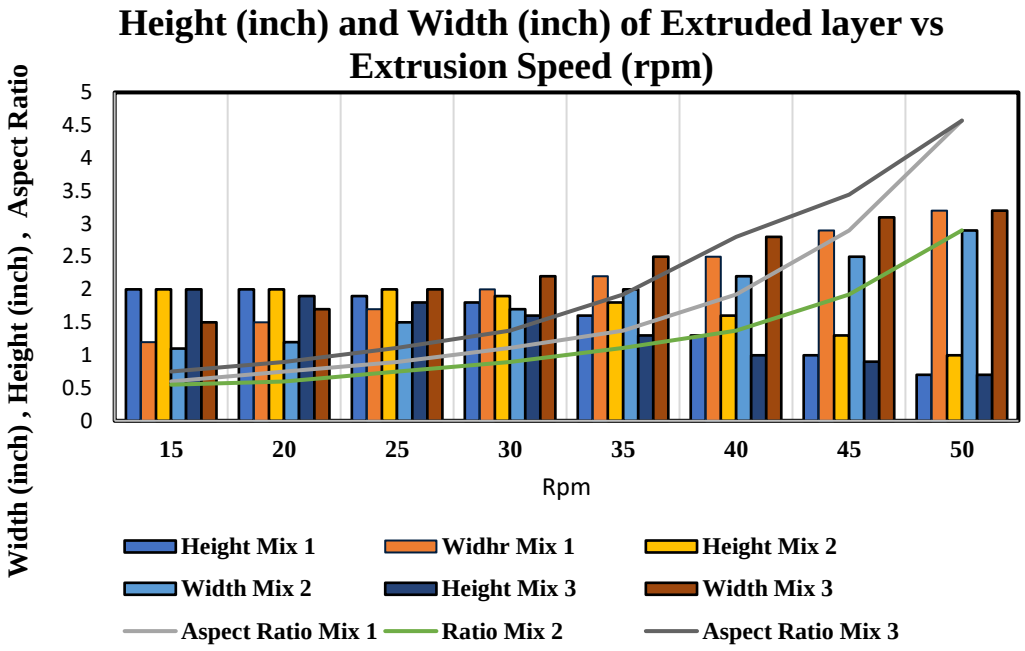

Figure 4.8: Evaluation of width and height of printed layer expressed in terms of aspect ratio and extrusion speed.

4.4. Results and Discussion:

So, the formulating of the 3D concrete printing required hit and trial experimentation to formulate the mix design. The mix design used included fibers (polypropylene), aggregate (retained on sieve with size 1/2"), Super plasticizer (polycarboxylate), water, sand, cement, and fly ash class f. Slump value of printability range is 2.5 inch to 6.5 inches. Below 2.5 inches no extrusion is observed and above 6.5 inches, there is no buildability of mix for printing. Deformation values are also noted with acceptable deformation range of 10% as per the literature and fixing linear speed at 32mm/sec this mix prints at extrusion speed of 35 rpm. Using the same speed, the following shapes were printed.

Figure 4.9: Printed Square with two layers upon each other.

4.10: Letters NUST printed with concrete printer and showcased at Independent Urdu Channel.

Chapter: 5 Machine Learning Based Mix Design Prediction

This chapter deals with the usage of various machine learning approaches to predict the mix design of printable concrete. The data set is selected from the literature and trained accordingly. The accuracy of predictions is assessed upon various criteria and validation is done using randomly selected mix design.

5.1 Introduction

This chapter focuses on 3D Concrete Printing, an advanced technology that offers promising opportunities for efficient and sustainable construction practices. 3D Concrete Printing offers numerous potential benefits compared to traditional concrete construction methods. However, a significant challenge lies in formulating a concrete mixture with the necessary mechanical and rheological properties, which often involves extensive experimentation and trial-and-error processes Overcoming this obstacle is crucial for the successful implementation of 3D Concrete Printing in real-world applications. Hence, the primary objective of this research is to explore a streamlined and less computationally intensive approach to developing a well-suited mixed design for printable concrete. Various researchers have already explored the application of machine learning techniques to predict concrete mix properties. Similarly, these techniques have been utilized to optimize concrete mix designs for 3D printing, employing methods such as Gaussian Process Regression, Decision Tree Regression, Support Vector Machine, and XGBoost Regression. In this chapter, we delve into the different machine-learning approaches employed for predicting and optimizing concrete mix designs in the context of 3D Concrete Printing. By analyzing the effectiveness of these techniques, we aim to contribute valuable insights into the

potential of machine learning to revolutionize the development of printable concrete mixtures, leading to more efficient and sustainable construction practices in the future.

5.2 Methodology

Various modelling approaches were considered for the analysis of the limited data set available. Artificial Neural Networks (ANNs) were initially explored for their potential to utilize multiple hidden layers and non-linear functions in modelling the output. However, due to the limited number of data samples, ANNs were deemed unsuitable as they are prone to overfitting when working with a small dataset (F. Rehman et al., 2022). One-dimensional Convolutional Neural Networks (CNNs) were also not considered since our dataset is not based on time series, and the parameters are not inherently related, requiring a high number of samples for effective modelling (Bolshakova et al., 2018). Autoencoders, which can compress inputs into a simplified code and reconstruct the input, were not chosen for regression analysis due to the limited size of the dataset, as they require a large amount of data to be effective (Kecman, 2005). Therefore, the current study conducted statistical analysis to understand the dataset's structure and shortlisted multiple regression models. Empirical experiments were then performed to determine the model that best captured the relations between the dependent and independent variables. The chosen model needed to handle complexity and non-linearity effectively. Four machine learning algorithms were selected: Support Vector Regression (SVR)(Kecman, 2005), Gaussian Process Regression (GPR) (Ebden, 2015), Decision Tree Regression (DTR) (Kotsiantis, 2013), and XGBoost (T. Chen et al., 2015). These algorithms were well-suited for modelling non-linear mappings and continuous nominal data, which were prevalent in the dataset.

The limited data availability influenced the choice of models, with SVR, XGBoost, and GPR being preferred due to their adaptability to smaller datasets. Though Decision Tree Regression requires

more data, pruning techniques were applied to mitigate this limitation, considering the relatively low variance in the dataset. All the selected models provided flexibility in parameter selection, enabling adjustments based on the available data to achieve optimal results. The methodology employed four machine learning algorithms suitable for continuous data, capable of capturing complex and non-linear relationships between dependent and independent variables. Figure 5.1 provides an overview of the research methodology, which involved studying two hardened state properties of printed concrete based on reliable datasets generated from the available literature. The concrete's bi-directional flexural strength was considered (directions 1 and 2 as shown in Figure 3), indicating its ability to resist bending moments in both longitudinal and transverse directions. Unidirectional tensile strength was also analyzed based on established testing methods (Panda et al., 2018; J. Zhang, Wang, & Gao, 2019).The limited availability of datasets in this research was attributed to the emerging and complex nature of the technology, limited adoption, ongoing active research, lack of standardized testing, and privacy concerns. The technology's emphasis on developing appropriate mix designs also led to a wide range of materials being utilized by researchers to determine optimal mix proportions.

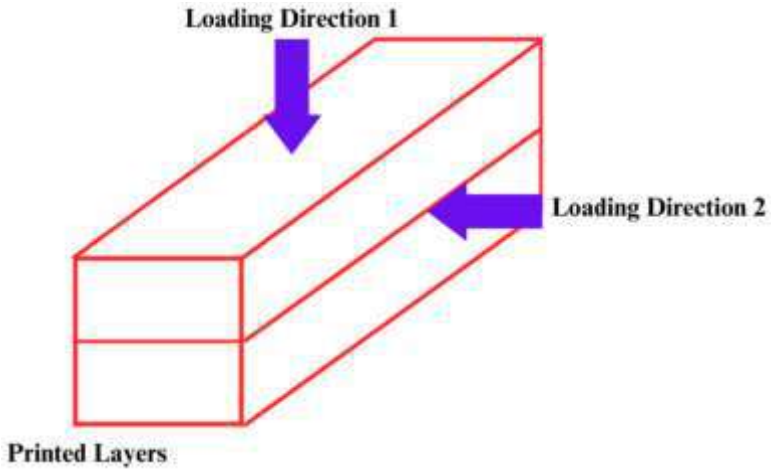

Figure 5.1: The anisotropic behavior of printed concrete in flexure was investigated in the same directions as those employed throughout the entire research study.

5.3 Regression through Machine Learning Approaches

In recent years, machine learning has proven to be a valuable tool in solving real-life problems, offering significant assistance in various domains (Sarker, 2021)The development of advanced concrete mixtures and their applications has necessitated the use of more precise and numerical models for predicting concrete properties. In concrete technology, researchers have widely utilized empirical and statistical models (Mohtasham Moein et al., 2023)

This study focuses on developing four distinct machine learning models to predict concrete's flexural strength and tensile strength. The chosen models include Decision Tree Regression, Support Vector Machine (SVM) Regressor, Gaussian Process Regressor, and Extreme Gradient Booster Regressor. Detailed descriptions of these machine learning models and their applications for predicting flexural and tensile strength can be found in the Supplementary Materials.

5.3.1Decision Tree Regressor

Decision Tree Regression is a versatile machine learning algorithm used to partition input data into smaller subsets. It effectively models data with non-linear or branched relationships between input features and target variables, enabling the establishment of decision rules to predict future outcomes (Kingsford & Salzberg, 2008). Decision Tree Regressor has been applied in concrete research to predict various properties, such as damage prediction in reinforced concrete, compressive strength prediction, and carbonation depth in concrete. Its capability to handle complex non-linear relationships between input variables and target variables makes it promising for accurately predicting properties in 3D concrete printing.

5.3.2Support Vector Machine Regressor (SVM)

Support Vector Machine Regression is a powerful supervised machine learning algorithm for

regression tasks. It fits the best possible line to produce continuous outputs for new input data (Dauji, 2016; Taffese et al., 2015). SVM regression involves mapping input data to a high-dimensional feature space through nonlinear mapping, followed by linear regression in this space. It effectively models complex non-linear relationships between input and output variables and has been widely used in concrete research due to its accurate and insensitive loss function (Sonebi et al., 2016; Yan & Shi, 2010) Its suitability for handling high-dimensional data and robustness to data noise makes SVM regression a valuable tool for predicting properties in 3D concrete printing.

5.3.3 Gaussian Process Regressor (GPR)

Gaussian Process Regressor is a non-probabilistic and non-parametric machine learning technique employed for regression analysis. Unlike Decision Tree Regression and SVM, GPR does not assume a unique functional form for modelling the dataset. Instead, it directly models the distribution of the data. GPR utilizes Bayesian inference to make predictions based on observed data. By assuming the output variable as a function of the input variable, GPR models it as a Gaussian Process. This probabilistic approach enables accurate modelling of complex non-linear relationships between input and output variables (Omidinasab et al., 2022a, 2022b; Słoński, 2011). In 3D concrete printing, GPR can be beneficial due to its robustness in handling limited data and noisy measurements, making it suitable for predicting various concrete properties.

5.3.4Extreme Gradient Booster Regressor (XG-Booster)

Extreme Gradient Booster Regression is a robust machine learning algorithm used for regression tasks. It is an ensemble method that combines multiple decision trees to make accurate predictions (T. Chen et al., 2015; Friedman, 2001). XG-Booster is known for its efficiency in handling large datasets and complex features, making it a popular choice in various applications (Nguyen-Sy et al., 2020). In concrete research, XG-Booster has been successfully used to predict high-

performance concrete's compressive and tensile strengths (Nguyen et al., 2021) .In the context of 3D concrete printing, XG-Booster's computational prowess and capability to handle complex features make it a valuable tool for predicting concrete properties, allowing for the optimization of the printing process and improved construction outcomes.

By leveraging these machine learning models, engineers and researchers can accurately predict the properties of 3D-printed concrete structures, leading to enhanced performance and cost reduction in the construction industry. The ability to optimize the printing process based on predicted properties allows for efficient adjustment of various parameters and settings to achieve desired performance characteristics. This study explores and compares this machine learning approach's effectiveness in predicting printed concrete properties, contributing to the advancement and implementation of 3D Concrete Printing technology.

5.4 Overview of Dataset

This study conducted a comprehensive analysis of a dataset comprising 77 mix designs for the development of a model predicting flexural strength (Bagheri & Cremona, 2020; Baz et al., 2022; Dwivedi et al., 2022; Hou et al., 2021a, 2021b; Kazemian et al., 2017; Lediga & Kruger, 2017; Z. Liu et al., 2019; Manikandan et al., 2020; Mohan et al., 2022; Muthukrishnan et al., 2022; Rahul et al., 2019; A. U. Rehman & Kim, 2021; Sahin & Mardani, 2022b, 2022a; Sanjayan & Nematollahi, 2019; Tripathi et al., 2022; Wang et al., 2022; Wongkornchaowalit & Lertchirakarn, 2011; C. Zhang et al., 2021)Additionally, 49 mix designs were examined to create a model for predicting tensile strength. The collected data from these mix designs were utilized to train and evaluate the accuracy of the models in predicting the flexural and tensile strengths of novel mix designs. The dataset encompasses various key components, including water, ordinary Portland cement, silica fume, fly ash, nano clay, Viscosity Modifying Agent (VMA), and coarse aggregate, with a maximum size of 10mm for the fine

aggregate, which is further classified based on a maximum size of 0.9mm and the type of sand used. Notably, the mix designs included in the dataset are fiber reinforced, and precise measurements of fiber quantity, type, tensile strength, Young's modulus, length, and diameter have been recorded. To gain insights into the printing process and its mechanical aspects, the dataset also incorporates information about the mechanical properties of the printer, such as the linear printing speed of the nozzle and nozzle correctional area. This information is valuable in understanding the impact of the printing technology's mechanical aspects on the properties of the printed concrete.

5.4.1 Details of Dataset

Cement

Cement plays a crucial role in concrete properties, with its dosage impacting various aspects. Higher cement dosage can lead to increased early age strength, but it may also result in higher heat of hydration and the formation of autogenous and drying shrinkage cracks (Lu et al., 2019; Shakor et al., 2019; Xu et al., 2021).

Fibers

Incorporating fibers into 3D Printing Concrete (3DPC) mixtures can significantly enhance printed parts' mechanical and physical properties. Fiber reinforcement can improve tensile and flexural strength, toughness, and crack resistance of 3DPC. However, careful consideration must be given to the choice of fiber type, content, and distribution to avoid potential adverse effects on printability and workability (Bos et al., 2019; Ding, Xiao, Zou, & Zhou, 2020; Van Der Putten et al., 2021; Zhou et al., 2023).

Fine Aggregate

Fine aggregate plays a vital role in 3D Printing Concrete mixtures to ensure strength and stability.

Fine aggregate particle size and shape impact rheological properties and printability, with smoother and more spherical particles improving flowability and reducing viscosity (Alexander & Mindess, 2005; Y. Chen et al., 2021; S. Yu et al., 2020). A higher percentage of sand can stiffen the material, negatively affecting extrudability and printability, highlighting the need for careful optimization of sand content and properties (Ding, Xiao, Zou, & Wang, 2020; Zou et al., 2021).

Coarse Aggregate

Coarse aggregate contributes positively to 3D Printing Concrete by enhancing its mechanical properties, reducing shrinkage, and lowering costs. However, the size and shape of the coarse aggregate can affect the mix's workability and extrudability, and larger particles may cause clogging in the printing nozzle (Rahul & Santhanam, 2020; C. Zhang et al., 2022).Therefore, meticulous selection and optimization of aggregate size and shape are essential to ensure optimal performance in 3D Printing Concrete.

Fly Ash

Fly ash, a by-product of coal-fired power plants, can partially replace cement in 3D Printing Concrete (3DPC) mixtures. Its incorporation can improve the workability, printability, and mechanical properties of 3DPC while reducing the environmental impact of concrete production (Marczyk et al., 2021)

Silica Fume

Silica fume serves as an additive in 3D Printing Concrete mixtures to enhance its properties, such as increasing compressive strength, reducing drying shrinkage, and improving durability. Additionally, it can reduce the heat of hydration and mitigate the risk of thermal cracking. However, its use may necessitate adjustments to the mix design and printing parameters (Brescia-Norambuena et al., 2021; Srinivas et al., 2022a).

Superplasticizer

Superplasticizers are employed in 3D Printing Concrete to improve workability, increase flowability, and reduce viscosity, resulting in enhanced extrudability and printing performance. They can also enhance the strength and durability of the final product by reducing the water-to-cement ratio and increasing the compactness of the concrete matrix. Nevertheless, excessive use of superplasticizers can lead to segregation and bleeding, affecting homogeneity and structural integrity (Qian et al., 2018; Different Effects of NSF and PCE Superplasticizer on Adsorption, Dynamic Yield Stress and Thixotropy of Cement Pastes, 2018).Therefore, proper dosage and selection of superplasticizers are critical for achieving desired properties in 3D Printing Concrete.

Accelerator

Accelerators are chemical additives used in 3D Printing Concrete mixtures to adjust working performance and achieve specific properties, such as increasing early age strength and decreasing setting time value. However, excessive use of accelerators can cause a rapid increase in the heat of hydration, leading to thermal cracks (Bhattacherjee & Santhanam, 2020; Wongkornchaowalit & Lertchirakarn, 2011).

5.4.2 Statistical Analysis of Data

Statistical analysis was conducted to gain insight into and interpret the datasets, specifically the output of X train. The describe() function provided a helpful starting point for exploring and understanding the training data, assisting in the selection of appropriate data preprocessing techniques and machine learning models. Table 5.1 below presents the range, mean, and standard deviation for the features of the dataset, focusing on flexural and tensile strength properties.

5.4.3 Data Cleaning

During this stage, the datasets for both properties underwent a thorough analysis to identify, correct, and eliminate any inconsistencies present. Missing data sets for Print Speed, Max Size, and Nozzle Area were handled by calculating the mean value and filling in the missing values accordingly.

5.4.4 Data Normalization

To enhance the accuracy of the models, data normalization was applied to both datasets. This process involved scaling the numerical features of the data set using Min-Max scaling. Equation 5.1 was utilized for data normalization:

$$x^* = \frac{x - x_{\min}}{x_{\min} - x_{\max}} \qquad 5.1$$

Here x* is the normalized value of the parameter, x is the original value, $x_{(min)}$ is the lowest value of that parameter, and $x_{(max)}$ is the highest value of the parameter.

Table 5.1 Statistical analysis of data set used for modelling purposes.

Parameters	Units	Range		Mean		Standard Deviation	
		Flexural Data	Tensile Data	Flexural Data	Tensile Data	Flexural Data	Tensile Data
Cement	Kg/m^3	207.61-2000	207.61-2000	581.83	674.87	361.57	438.79
Water	Kg/m^3	130.9-760	135-760	263.85	327.32	155.58	176.37
Silica Fume	Kg/m^3	0-293	0-280	82.09	55.94	97.94	91.51
Fly ash	Kg/m^3	0-1380	0-1380	272.84	321.27	345.58	446.78

HRWA	Kg/m^3	0-36	0-36	6.39	5.68	7.53	8.79
Accelerator	Kg/m^3	0-146.4	0-146.4	4.5	2.99	19.84	20.91
Nano Clay	Kg/m^3	0-5.89	0-5.89	0.6	0.51	1.58	1.51
VMA	Kg/m^3	0-38.64	0-31.74	2.39	3.78	6.15	10.41
Coarse Aggregate Amount	Kg/m^3	0-1566.3	0-1566.3	189.72	241.16	392.25	494.08
Coarse Aggregate Size	mm	0-10	0-10	1.75	1.62	2.84	3.37
Fine Aggregate	Kg/m^3	195.7-3420	195.7-3420	838.48	836.09	593.23	721.23
Fine Aggregate Size	mm	0.176-3	0.2-3	0.45	0.53	0.2	0.42
Tensile Strength of Fibers	MPa	300-3000	300-3000	1775.8	1564.4	997.5	1087.31
Young Modulus of Fibers	GPa	3-200	3-300	68.48	71.42	67.94	61.48
Amount of Fibers	Kg/m^3	1-157	1.96-157	23.44	13.57	38.64	15.28
Length of Fibers	mm	6--23	6---23	10.47	10.35	4.66	5.36
Diameter of Fibers	µm	11.2-200	11.2-300	47.3	31.59	56.05	38.5
Print Speed	mm/sec	10-450	10-120	94.22	63.72	109.68	31.55
Nozzle Area	mm^2	50.25-1259	78.54-1256	546.58	580.16	365.87	351.18

5.5 Evaluation Criteria

Two distinct sets of evaluation criteria were established to assess the regression models' accuracy. In a recent study, mixtures were evaluated based on their flexural strength when cast and printed in both directions, 1 and 2, as well as their tensile strength. For the flexural strength model, 57 mix designs were used for training, and the model's performance was subsequently evaluated on 20 additional mix designs in a 3:1 ratio. For the tensile strength model, 35 mix designs were used for training, and 14 were used for testing.

5.5.1 Mean Square Error (MSE)

The Mean Square Error (MSE) was employed to evaluate the regression models by measuring the average squared magnitude of errors generated by the models. A higher MSE value indicates that the model's predictions are, on average, less accurate, with a larger average squared magnitude of errors between the predicted values and the actual values of the target variable. The MSE is calculated using the formula:

$$MSE = \frac{1}{n}\sum_{i=1}^{n}(Y_{pre} - Y_{actual})^2 \quad (5.2)$$

5.5.2 Coefficient of Determination (R-Squared/R2)

The Coefficient of Determination, denoted as R2, was utilized to evaluate the regression models based on the statistical measure of the portion of variations in the dependent variable predicted from the independent variable(s) through regression models. R2 values lie between 0 and 1, with 1 indicating that all variations in the dependent variable can be explained by the independent variable(s), while 0 indicates that none of the variations can be explained. A value between 0 and 1 represents the proportion of the variance in the dependent variable explained by the independent variable(s). The formula to calculate R2 is as follows:

$$R^2 = \frac{\sum_{i=1}^{n}(Y_{pre} - \overline{Y_{pre}})}{\sum_{i=1}^{n}(Y_{actual} - \overline{Y_{actual}})} \quad (5.3)$$

5.5.3Mean Absolute Error (MAE)

Mean Absolute Error (MAE) is a commonly used metric in regression analysis to measure the accuracy of a regression model's predictions. It calculates the average difference between the predicted and actual values of the dependent variable. A lower MAE value indicates more accurate predictions, while a higher MAE value suggests less accuracy. MAE is calculated using the formula:

$$MAE = \frac{\sum_{i=1}^{n} |y_i - x_i|}{n} \quad (5.4)$$

5.5.4Root Mean Square Error (RMSE)

Root Mean Square Error (RMSE) is another commonly used metric to measure the difference between predicted and actual values in statistical analysis and machine learning. It is the square root of the average squared differences between predicted and actual values. A lower RMSE value indicates better accuracy in the model's predictions. RMSE is calculated using the formula:

$$MSE = \sqrt{\frac{1}{n}\sum_{i=1}^{n}(Y_{pre} - Y_{actual})^2} \quad (5.5)$$

5.6 Hyperparameter Tuning

Hyperparameter tuning involves finding the best combination of hyperparameters for a machine-learning algorithm to achieve optimal performance. These settings affect the behavior and performance of an algorithm and cannot be learned from the data. To optimize the performance of

the linear regression model, hyperparameters were tuned to identify the best possible values. The optimal values of hyperparameters are shown in Table 5.2 and Table 5.3 In multiple training cases, the optimal values are indicated in bold. Hyperparameter tuning is essential for achieving cutting-edge outcomes and improving a model's accuracy and generalization capabilities.

The hyperparameters are shown below:

In optimizing the regression model's performance for predicting flexural strength, hyperparameter tuning was conducted, and the results are presented in Table 3.3. Hyperparameter tuning involves systematically searching for the best combination of hyperparameters to achieve the most accurate and effective model. These hyperparameters play a crucial role in shaping the behavior and performance of the model. The optimal values were identified through a rigorous evaluation of different hyperparameter settings, ensuring that the model is fine-tuned to capture the complex relationships between the input variables and the flexural strength of the 3D-printed concrete. By selecting the best hyperparameters, the model's accuracy and generalization capabilities were significantly improved, enabling it to provide more reliable predictions of flexural strength for different mix designs. The success of hyperparameter tuning in Table 5.3 underscores its importance in enhancing the performance and predictive capabilities of the regression model for flexural strength, ultimately contributing to the advancement and successful implementation of 3D concrete printing technology in construction applications.

Table 5.2: Tensile strength model's hyperparameters.

Tensile Strength					
		Test			
		Direction 1			
Model	**Hyperparameter**	**R2_score**	**RMSE**	**MSE**	**MAE (MPA) (MPa)**
DecisionTreeRegressor	**Default parameters:** criterion='squared_error', splitter='best', max_depth=None, min_samples_split=2, min_samples_leaf=1	0.7217	1.0904	1.1889	0.5857
XG Boost Regressor	**Default parameters:** loss='squared_error', learning_rate=0.1, n_estimators=100, subsample=1.0, criterion='friedman_mse', min_samples_split=2	0.6757	1.1771	1.3856	0.6255
Gaussian Process Regressor	**Default parameters / NA**	-0.8156	2.7853	7.7583	1.7688
SVM Regressor	**Parameters:** Kernel = "linear"	**0.8893**	**0.6877**	**0.4729**	**0.5168**

Kernel = “rbf”		0.7363	1.0614	1.1265	0.7923
Kernel = “sigmoid”		0.4781	1.4933	2.2299	1.0734
Kernel = “poly”	degree=2	0.8697	0.7461	0.5567	0.5619
	degree=3	0.8705	0.7436	0.5529	0.5294
	degree=4	0.8726	0.7377	0.5443	0.5230
	degree=5	0.8454	0.8126	0.6603	0.6108
	degree=7	0.5856	1.3306	1.7705	0.9655

5.7 Results and Discussion

Based upon hyperparameters, the results are discussed below. Using the datasets for both flexural and tensile models, various techniques were employed to train the models, and their accuracy was evaluated based on two metrics: Mean Square Error (MSE) and Coefficient of Determination (R2). A lower MSE value indicates higher accuracy of the model's predictions, while the R2 value, ranging from 0 to 1, signifies the model's ability to predict the target variable. An R2 value of 1 indicates a perfect prediction, while a value of 0 implies that the model fails to explain the variance in the dataset. Generally, higher R2 values indicate that the model performs better in explaining the variation in the target variable. The results obtained from these evaluations demonstrated a high level of excellence and surpassed the outcomes of previous research studies, making them highly suitable for predictive purposes. To visually compare the model's predictions with the actual data, graphical representations have been provided in the figures below, offering a detailed comparison between the two.

Table 5.3 Hyperparameters for the modeling of the flexural strength

Flexural Strength												
Model	**Hyperparameter**	**Test**										
		Casted				**Direction 1 (MPA)**				**Direction 2 (MPA)**		
		R2_score	*RMSE*	*MSE*	*MAE (MPA)*	R2	*RMSE*	MSE	MAE (MPA)	R2	*RMSE*	*MSE*	*MAE (MPA)*
Decision Tree Regressor	**Default parameters:** criterion='squared_error', splitter='best', max_depth=None, min_samples_split=2, min_samples_leaf=1	0.7107	4.0378	16.3038	2.1685	0.7253	4.2234	17.8378	2.1450	0.7166	3.6106	13.0370	1.9234
XG Boost Regressor	**Default parameters:** loss='squared_error', learning_rate=0.1, n_estimators=100, subsample=1.0,	0.7826	3.4995	12.2471	1.9138	0.8571	3.0464	9.2805	1.6562	0.8237	2.8478	8.1100	1.6802

	criterion='friedman_mse', min_samples_split=2											
Gaussian Process Regressor	**Default parameters / NA**	0.8586	2.8223	7.9658	1.7799	0.8997	2.5521	6.5136	1.6653	0.8919	2.2298	4.9724	1.5179
	Parameters: Kernel = “linear”	0.8389	3.0131	9.0789	2.2241	0.8302	3.3203	11.0248	2.3213	0.8588	2.5482	6.4936	1.8319
	Kernel = “rbf”	0.3747	5.9361	35.2376	3.4569	0.3441	6.5263	42.5938	3.7748	0.4109	5.2057	27.0992	3.1575
	Kernel = “sigmoid”	0.2753	6.3902	40.8355	3.8144	0.2507	6.9757	48.6608	4.2864	0.2992	5.6780	32.2397	3.5497
SVM Regressor	Kernel = “poly” degree=2	0.8015	3.3440	11.1820	2.3023	0.7940	3.6570	13.3741	2.4048	0.8556	2.5772	6.6422	1.8418
	Kernel = “poly” degree=3	0.8798	2.6020	6.7705	1.8348	0.8681	2.9266	8.5651	1.9164	0.8650	2.4914	6.2070	1.7467
	Kernel = “poly” degree=4	0.8947	2.4357	5.9326	1.5969	0.8824	2.7630	7.6342	1.7180	0.8705	2.4408	5.9577	1.6728
	Kernel = “poly” degree=5	**0.9009**	**2.3629**	**5.5837**	**1.5843**	**0.8936**	**2.6284**	**6.9089**	**1.6899**	**0.8785**	**2.3643**	**5.5900**	**1.6301**
	Kernel = “poly” degree=7	0.8597	2.8119	7.9068	1.8643	0.8621	2.9921	8.9529	2.012	0.8713	2.4331	5.9202	1.7

5.7.1 Decision Tree Regressor

In the case of Decision Tree Regression, the model was constructed using default parameters, such as criterion = 'squared_error', splitter = 'best', max_depth = None, min_samples_split = 2, and min_samples_leaf = 1. This Decision Tree model was utilized to evaluate the flexural strength and tensile strength of various mix designs in the study. For the flexural strength evaluation, the model was trained on an input dataset, employing the default 'squared_error' criterion to assess the quality of splits in the decision tree. The best splitter strategy was employed to select the optimal split among all potential splits, while the default max_depth parameter enabled the tree to expand until all leaves were pure or contained fewer than the default value of 2 samples. Additionally, the min_samples_leaf parameter was set to its default value of 1, determining the minimum number of samples required to form a leaf node. The same strategy and parameters were applied in the case of tensile strength modeling. The trained and tested values and 10% error lines for data scattering are depicted in Figure 5.2.

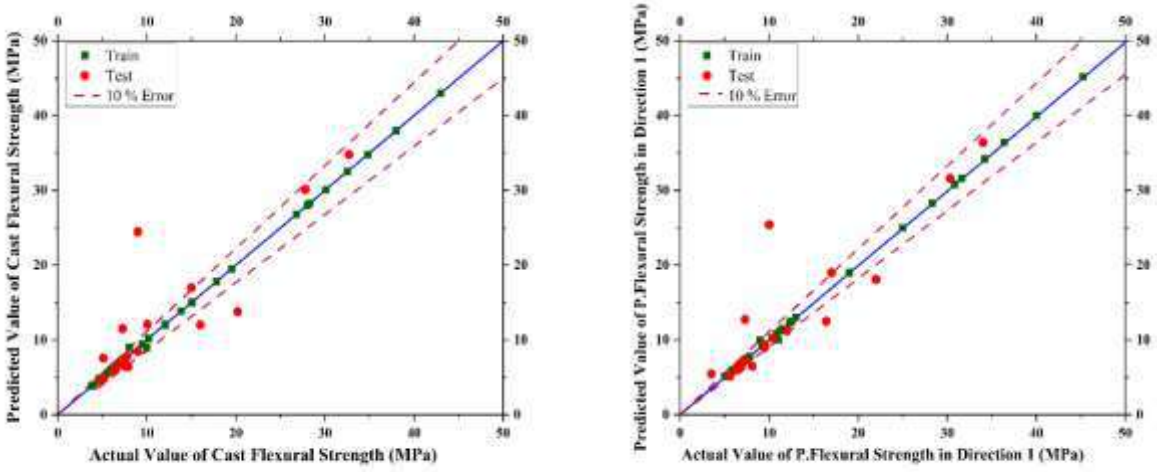

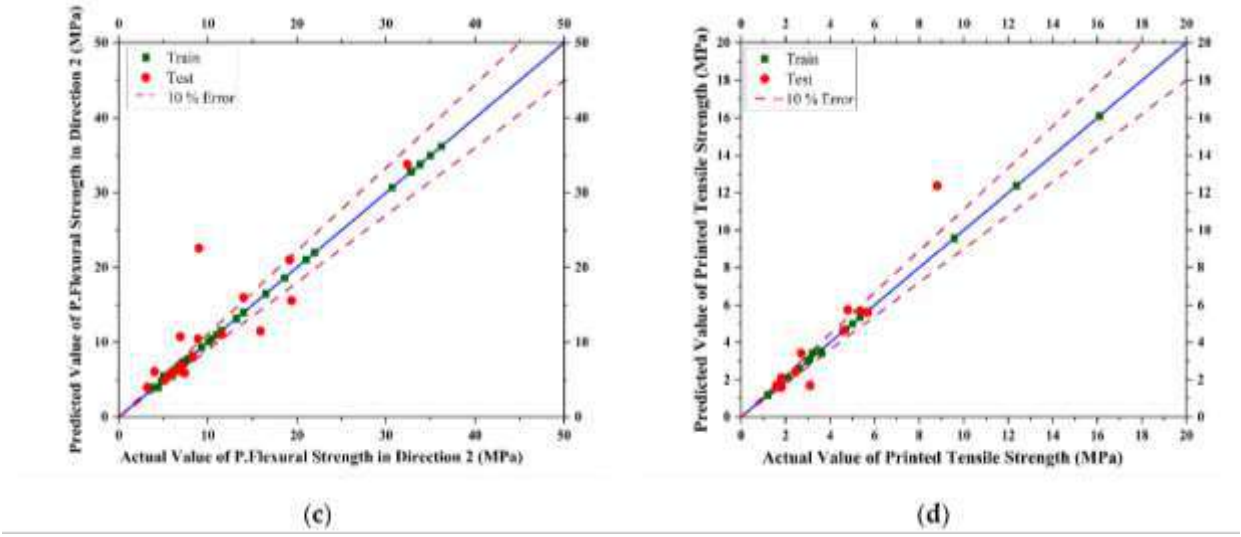

Figure 5.2. Graphical representation of the actual versus predicted results obtained from the Decision Tree Regression model for different scenarios: (a) Casted Flexural Strength, (b) Printed Flexural Strength in Direction 1, (c) Printed Flexural Strength in Direction 2, and (d) Printed Tensile Strength of concrete. The curves visually demonstrate how well the model's predictions align with the actual values for each specific case, providing valuable insights into the model's performance for the different types of strength evaluation.

5.7.2 Support Vector Machine (SVM)

The Support Vector Machine (SVM) model was employed to predict mixtures' flexural and tensile strength based on their composition. SVM utilizes kernel functions, which play a crucial role in determining the shape of the decision boundary used to separate different classes in the regression problem. This study utilized three kernel functions: linear, Radial Basis Function (RBF), and sigmoid kernels. To evaluate the SVM model's performance, the models were trained and tested using five levels of degrees in modelling. The degree of the polynomial kernel function directly impacts the complexity of the decision boundary, with higher degrees allowing for more intricate decision boundaries. Specifically, degrees 2, 3, 4, 5, and 7 were utilized in this analysis. The

optimum degree for the polynomial kernel function was determined based on the established evaluation criterion. The trained values and tested values with 10% error lines, depicting data scattering, are visually presented in Figure 5.3. This graphical representation allows for a detailed examination of the model's accuracy in predicting flexural and tensile strengths for different scenarios, considering various degrees of the polynomial kernel function.

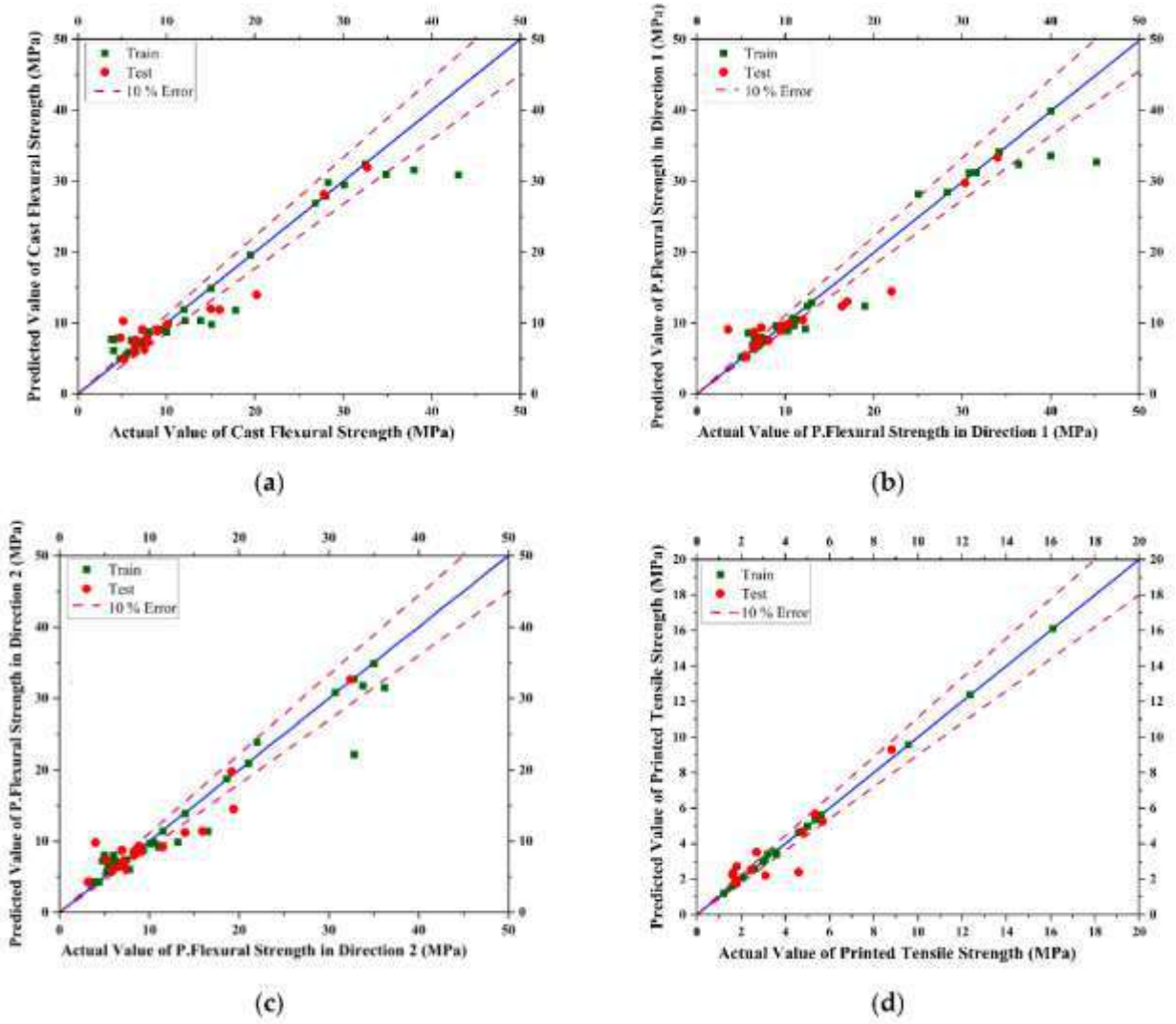

Figure 5.3 Graphical representation of the actual versus predicted results obtained from the Support Vector Machine model for different scenarios: (a) Casted Flexural Strength, (b) Printed Flexural Strength in Direction 1, (c) Printed Flexural Strength in Direction 2, and (d) Printed

Tensile Strength of concrete. The curves visually demonstrate how well the model's predictions align with the actual values for each specific case, providing valuable insights into the model's performance for the different types of strength evaluation.

5.7.3 Gaussian Process Regressor

The Gaussian Process Regressor (GPR) was used to train and test the dataset. The trained values and tested values, along with 10% error lines to indicate data scattering, are visually represented in Figure 5.4. It showcases the actual versus predicted results for the Gaussian Process Regressor model for various scenarios, including Casted Flexural Strength, Printed Flexural Strength in Direction 1, Printed Flexural Strength in Direction 2, and Printed Tensile Strength of Concrete. The graphical representation allows for a comprehensive assessment of the model's performance in predicting these specific strengths, providing valuable insights into the accuracy of the Gaussian Process Regressor in handling the given dataset.

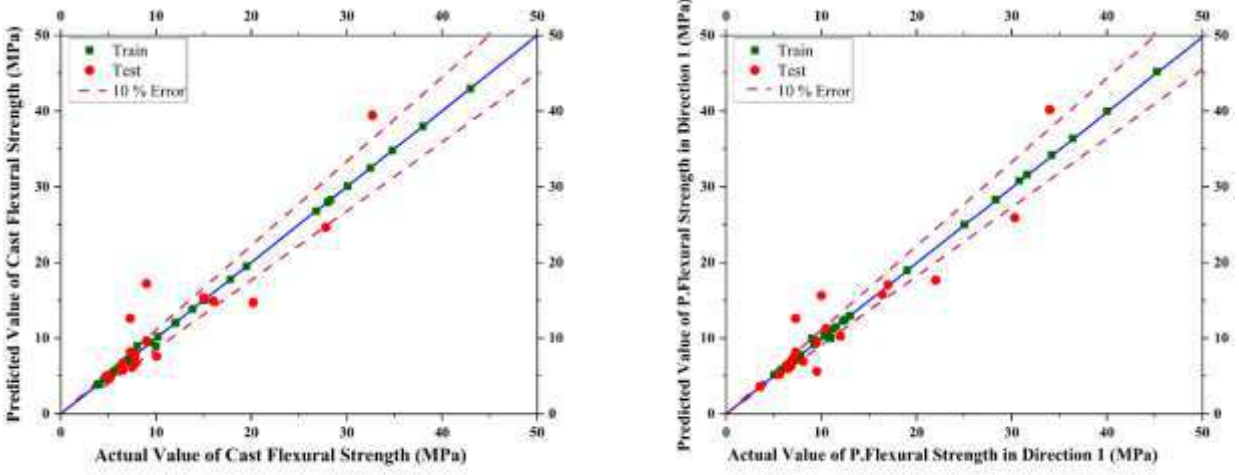

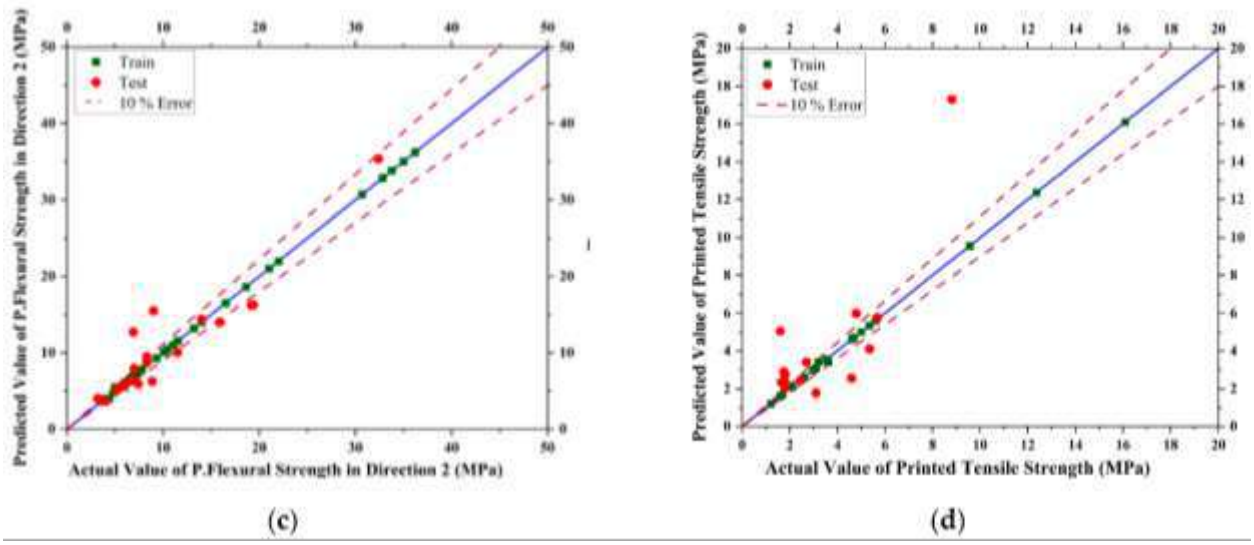

Figure 5.4 Graphical representation of the actual versus predicted results obtained from the Gaussian Process Regressor model for different scenarios: (a) Casted Flexural Strength, (b) Printed Flexural Strength in Direction 1, (c) Printed Flexural Strength in Direction 2, and (d) Printed Tensile Strength of concrete. The curves visually demonstrate how well the model's predictions align with the actual values for each specific case, providing valuable insights into the model's performance for the different types of strength evaluation.

5.7.4 XGBOOST Regressor

The XGBOOST Regressor, a gradient-boosting regression model, was implemented using the sci-kit-learn Python library. This model played a pivotal role in predicting the flexural and tensile strength of various mixtures based on their composition. During the training phase, the model was optimized using the mean squared error loss function, with a learning rate of 0.1. To build the ensemble model, 100 trees were utilized, and each tree was fitted on a specific subset of the data, as defined by the subsample parameter, with a default value of 1.0.

To evaluate the quality of each split in the decision tree, the Friedman mean squared error criterion was employed, having a default value of 'friedman_mse'. Additionally, the min_samples_split

parameter was adjusted to control the minimum number of samples required to split an internal node, with the default value set to 2. To accurately assess the model's performance, a portion of the available data was reserved for testing, while the remaining data was used for training purposes. Consequently, both the flexural strength and tensile strength models were trained and evaluated on their respective datasets. The trained values and tested values, along with 10% error lines to visualize data scattering, are illustrated in figure 5.5 below. This comprehensive representation allows for an in-depth analysis of the XGBOOST Regressor's predictive capabilities for both flexural and tensile strength predictions.

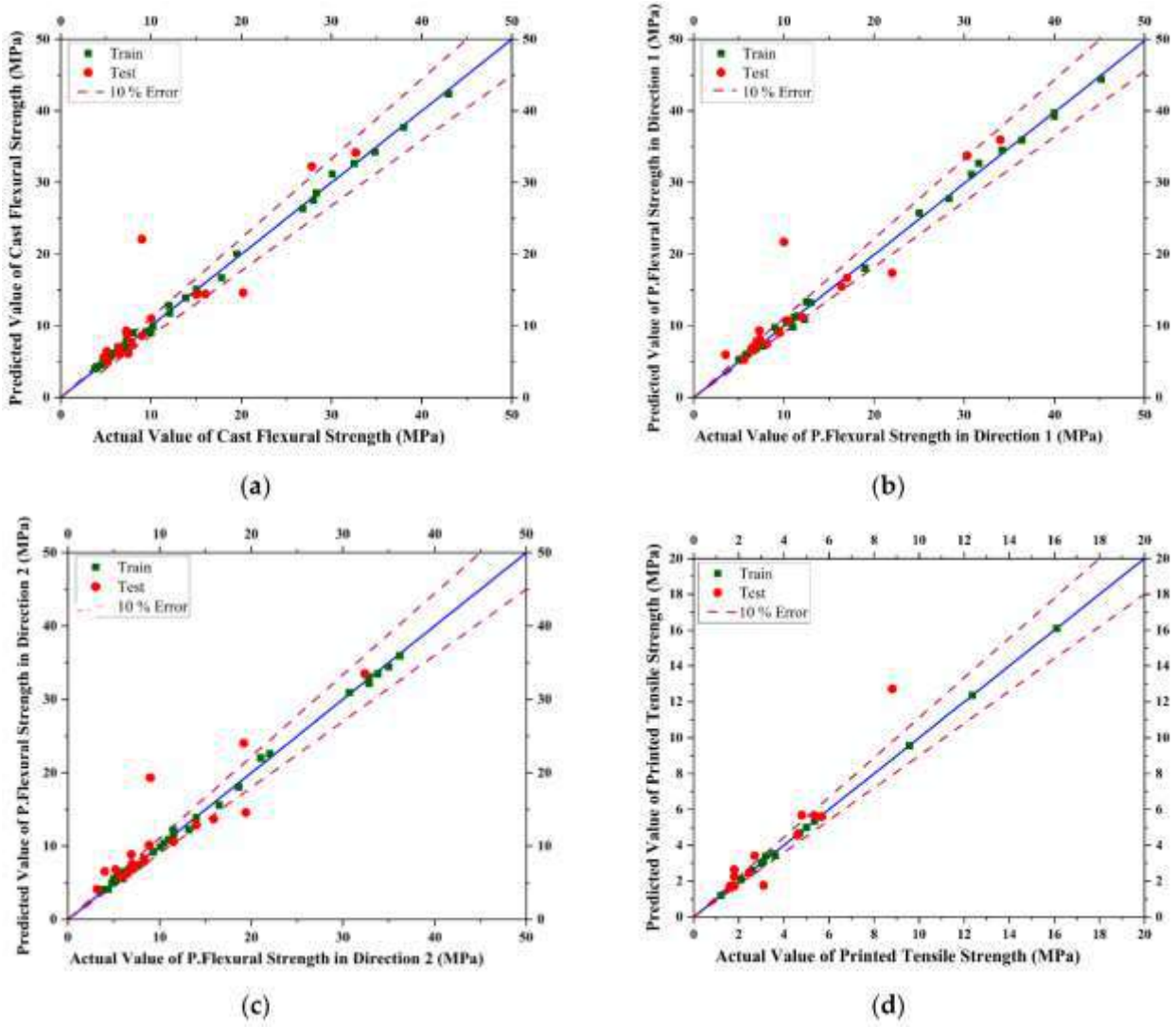

Figure 5.5 Graphical representation of the actual versus predicted results obtained from the XGBoost Regression model for different scenarios: (a) Casted Flexural Strength, (b) Printed Flexural Strength in Direction 1, (c) Printed Flexural Strength in Direction 2, and (d) Printed Tensile Strength of concrete. The curves visually demonstrate how well the model's predictions align with the actual values for each specific case, providing valuable insights into the model's performance for the different types of strength evaluation.

The study involved a comprehensive comparison of various machine learning algorithms and their performance in predicting the difference between predicted and actual values. The hyperparameter tuning section presented a detailed analysis of how different hyperparameters impact the model's results, highlighting the contrast between each algorithm's R2 and RMSE values. The SVM algorithm emerged as the best performer, achieving remarkable R2 and RMSE values. Empirical analysis with different hyperparameters further fine-tuned the SVM model's results. For predicting tensile strength, the linear kernel yielded excellent outcomes with an R2 of 0.8454, an MAE of 0.6108, an MSE of 0.6603 MPa, and an RMSE of 0.8126. Meanwhile, for flexural strength, the poly kernel of degree 5 produced outstanding results with R2 values of 0.9009, 0.8936, and 0.8785 for Casted, Direction 1, and Direction 2, respectively. The corresponding MAE, MSE, and RMSE values were 1.5843, 1.689, and 1.6301 for Casted, Direction 1, and Direction 2, respectively. SVM's ability to handle high-dimensionality data and model complex non-linear relationships made it an excellent choice for the prediction task.

On the other hand, the Decision Tree Regressor and XGBoost Regressor, though capable of modelling relations between discrete data or non-linear attributes, showed a higher risk of overfitting. While these algorithms produced optimal results on the training data, they failed to generalize effectively and yielded unsatisfactory results on the test set. The Decision Tree

Regressor achieved R2 scores of 0.72036 and 0.67230 for tensile and RMSE values of 1.09311 MPa and 1.18332 MPa for tensile and XGBoost Regressor, respectively, indicating inferior performance compared to SVM. In the case of flexural strength, the Gaussian Process Regressor demonstrated comparable results to the best performing SVM model, with R2 values of 0.8265, 0.87778, and 0.8673 for Casted, Direction 1, and Direction 2, respectively, along with corresponding RMSE values of 3.1262 MPa, 2.8174 MPa, and 2.4701 MPa. However, the Gaussian Process Regressor performed poorly on the tensile dataset, with an R2 of -0.61268 and an RMSE of 2.62509 MPa. This disparity could be attributed to the Gaussian Process Regressor's non-parametric nature, relying heavily on data, and possibly facing limitations due to insufficient data for the tensile prediction. Overall, the study showcased the strengths and weaknesses of various machine learning algorithms, with SVM standing out as the most robust and accurate model for the given prediction task.

5.8 Validation of Models

Validation of the predictive models was crucial to ensure their reliability and generalizability. While the models exhibited exceptional performance during the training phase using comprehensive data, it was essential to assess their accuracy on entirely new data, which could be either part of the dataset or entirely different. For this purpose, six mixed designs were carefully selected from the dataset for validation, as presented in Table 5.4 and Table 5.5. The validation process results, as depicted in Figure 5.6, indicated that the model's accuracy evaluation criteria remained superior. No prior instance of this specific model being trained on 3D concrete printing existed in the available literature. Despite this novelty, the findings demonstrated that the model's performance remained robust and dependable even when tested on novel data from the dataset. This validation process further solidified the models' credibility and

their potential applicability in real-world scenarios.

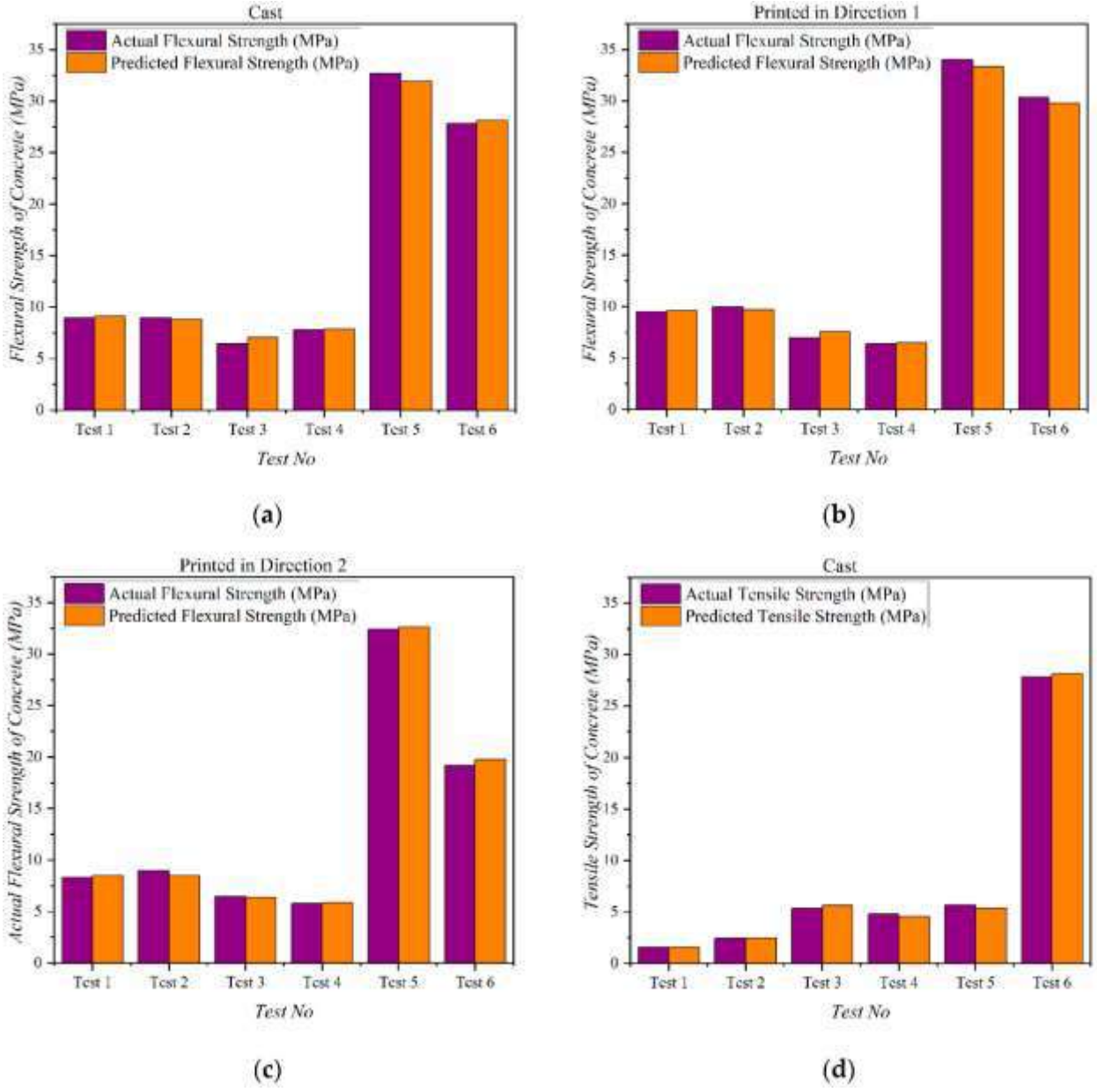

Figure 5.6 Comparison of the forecasted outcomes for different aspects of strength evaluation can be observed as follows: (a) Casted Flexural Strength (b) Printed Flexural Strength in Direction 1 (c) Printed Flexural Strength in Direction 2 (d) Printed Tensile Strength of Concrete.

Table 5.4 Mix designs used for validation of tensile strength model.

Tensile Strength Test Mix					
Mix	**1**	**2**	**3**	**4**	**5**
Water (kg/m^3)	289.7	256	329.8	177.12	135.19
Cement (kg/m^3)	783	562	565.37	656	207.61
SF (kg/m^3)	39.15	81.4	0	246	0
FA (kg/m^3)	140.9	162	671.38	118	275.21
HRWA (kg/m^3)	0.98	4.8	14.13	3	5.79
Nano Clay/Nano Clay	0	0	5.89	0	2.414
VMA (kg/m^3)	0.49	2.41	1.18	0	0.48
Max Size (mm)	10	0	0	0	0
Amount Fine Aggregate (kg/m^3)	978.7	1144	471.14	455	275.21
Max Size (mm)	0.39	0.4	0.3	0.31	0.2
Sand Type	River Sand	Malmmesbury	Silica Sand	Silica Sand	Silica Sand
Fiber	PP	PP	PE	PE	PE
Tensile Strength MPa	300	300	300	2900	3000
Young's Modulus (GPA)	3	3	116	116	116
Amount (kg/m^3)	1.96	22	40	10	14.55
Length (mm)	12	6	12	23	12
Diameter (micrometer)	130	30	24	25	24
Print Speed mm/sec	100	60	100	10	100
Nozzle Area mm^2	1256	490.625	314	1000	314

Table 5.5 Mix designs used for validation of flexural strength model.

Flexure Strength Test Mix						
Mix	**1**	**2**	**3**	**4**	**5**	**6**
Water (kg/m^3)	244	285	210	240	156	154
Cement (kg/m^3)	376	289	350	622	273	750
SF (kg/m^3)	41.36	145	100	88.9	293	165
FA (kg/m^3)	100	277	185	257	0	0
HRWA (kg/m^3)	5.64	9	8	2.57	18	10
Nano Clay/Nano Clay	0	0	0	0	5	0
VMA (kg/m^3)	0	0	4	0	0	1.08
Coarse Aggregate Amount (kg/m^3)	0	0	0	0	390	180
Size	0	0	0	0	4.75	4.75
Amount Fine Aggregate (kg/m^3)	732.6	1209	750	1066.75	878	924
Max Size (mm)	0.4	0.47	0.8	0.38	0.176	0.85
Sand Type	Silica Sand	Malmesbury	Midas sand	River Sand	Silica Sand	Quartz Sand
Fiber	PVA	Glass	PP	PP	Steel	Steel
Tensile Strength MPa	1600	450	300	3000	2500	2500
Young's Modulus (GPA)	30	74	3.85	3	200	200
Amount (kg/m^3)	7	13.5	12.7	1.2	157	39
Length (mm)	18	6	6	9	6	10
Diameter (micrometer)	39	40	30	23	200	0.12
Print Speed mm/sec	110	150	0	450	30	15
Nozzle Area mm^2	112.32	50.25	625	240	706.5	176.625
Casted	9	9	6.5	7.8	32.7	27.81
Direction 1 (MPa)	9.5	10	7	6.4	34	30.32
Direction 2 (MPa)	8.3	9	6.5	5.8	32.4	19.17

5.9 Discussion

ML-based predictive models for the flexural and tensile strength of 3D-printed concrete have been scarce in the literature. Therefore, the objective of this study was to create a precise ML-based predictive model for the anisotropic flexural and printed tensile properties of concrete, considering both cast and printed scenarios. The data collected from various sources was used to train, validate, and test four distinct predictive models based on ML techniques, namely Decision Tree Regression, Support Vector Machine (SVM) Regressor, Gaussian Process Regressor, and Extreme Gradient Booster Regressor.

The primary research outcomes are as follows:

- Among the four models, the Support Vector Machine Regression-based predictive model demonstrated the highest degree of accuracy compared to the others, such as Decision Tree Regressor, Gaussian Process Regressor, and Extreme Gradient Booster Regressor.
- For the printed flexural strength in both Direction 1 and Direction 2, the SVM model achieved the highest Coefficient of Determination (R2_score) of 0.8936 and 0.8785, respectively. On the other hand, the R2 scores for the other models were lower, indicating less accurate predictions.
- The evaluation criteria, including RMSE, MSE, R2, MAE, and Sensitivity Analysis, consistently pointed to the SVM Regression Model as the most accurate among the tested techniques.
- The SVM model provided a robust and dependable performance even when tested on novel data from the dataset, indicating its reliability for predictive purposes.

In this study, we encountered the challenge of a small sample size, which could lead to overfitting

during model training. Different regression methods were evaluated, and it was observed that Decision Tree Regressor and Extreme Gradient Boosting Regressor tended to overfit due to their reliance on the dataset. Gaussian Process Regressor, on the other hand, could capture noise in the data, leading to overfitting. In contrast, the SVM Regressor performed better, owing to its ability to transform data into higher-order planes through kernel transformations and find a function for the relationships between variables. The regularization term in SVM helped lower the risk of overfitting, making it more suitable for limited sample sizes and high-dimensional spaces.

In conclusion, the developed ML-based predictive model offers accurate estimates of the flexural and tensile strength of 3D-printed concrete. This model has significant implications for the construction industry, allowing for efficient ingredient selection without laborious laboratory trials. Moreover, its accurate predictions can enhance the structural integrity of 3D-printed concrete structures, ensuring their safety and longevity. Overall, this predictive model has the potential to revolutionize the construction industry by enabling efficient and cost-effective production of 3D-printed concrete structures.

Chapter 6: Conclusion and Discussions

6.1 Conclusion and Discussions

The following conclusion can be drawn from this project.

1. The Development of Indigenous Concrete Printer and Mix Design project represents a groundbreaking initiative that has the potential to revolutionize the construction industry in Pakistan. By integrating cutting-edge technologies such as the Indigenous Concrete Printer and machine learning-based mix design optimization, the project opens new avenues for enhanced construction processes, improved structural design, and resource efficiency.
2. The fabrication of concrete printer involved using locally available raw materials. The printer is fabricated by first developing a frame of required size, then developing an extruder with an auger blade modified to our requirement, developing a control system for movement of extruder in three axis and assembling all the components.
3. The formulation of mix design involves selecting locally available constituents like cement, sand, fibers (polypropylene), aggregate, super plasticizer, and fly ash. The mix design is formulated and assessed in terms of fresh state properties and suitable printability.
4. Printing of layer upon layer and various alphabetical shapes were done to prove this design concept.
5. Various Machine Learning approaches were used to predict the mix design like Support Vector Machine, Gaussian Process Regressor, Decision Tree Regression and XGBoost Regression. The models were trained and evaluated in terms of the various criteria like R2, RMSE, MSE and MAE.

6. In Machine learning integration, Support Vector Machine outperforms all other models. In the case of printing in Direction 1, the Coefficient of Determination (R2_score) for SVM is 0.8936, while for DTR, GPR, and XGBoost, it is 0.7253, 0.8997, and 0.8571, respectively. Similarly, for printing in Direction 2, the Coefficient of Determination (R2_score) for SVM is 0.8785, while for DTR, GPR, and XGBoost, it is 0.7166, 0.8919, and 0.8237, respectively. The higher R2 value obtained with SVM indicates a better fit of the data to the regression model compared to other techniques. The R2 values reported in this research are in line with previous findings, where values of 0.84, 0.94, 0.945, and 0.92 were reported.
7. The uniqueness of the project lies in its integration of the Indigenous Concrete Printer and machine learning-based mix design. This combination sets it apart as the first-of-its-kind initiative in Pakistan, showcasing the potential for innovation and technological advancement in the construction sector. As a result, the project serves as an inspiring example for other industries and innovators, encouraging them to adopt advanced technologies and push the boundaries of their respective fields.

6.2 Future Recommendations

The mechanical and rheological properties of mix designs are comparable to the properties available in the literature. In the future, the Development of the Indigenous Concrete Printer and Mix Design project should focus on large-scale implementation and advancement to fully realize its potential. Collaborating with the construction industry and key stakeholders will be essential to showcase the effectiveness and practicality of the Indigenous Concrete Printer and machine learning-based mix design in real-world construction projects. Conducting pilot projects in diverse construction settings will serve as case studies, validating the project's

efficiency and adaptability.

As artificial intelligence (AI) continues to evolve rapidly, integrating more advanced AI algorithms and techniques into the project can further enhance its capabilities. Exploring cutting-edge AI approaches, such as deep learning and reinforcement learning, can lead to an even more sophisticated mix design predictions and printer control systems. Developing real-time monitoring and control systems for the Indigenous Concrete Printer will improve its responsiveness and reliability during the construction process, optimizing construction efficiency.

Expanding the printer's capabilities to include multi-material printing can enable the construction of stronger and more sustainable structures. Researching and integrating various materials, such as fibers, geopolymers, and recycled aggregates, will open up new possibilities for innovative construction designs. Collaborating with international research institutions and construction companies can provide access to global expertise and best practices, accelerating the project's progress and fostering knowledge exchange.

Investing in training and skilling programs for construction professionals and workers will ensure the successful adoption of the Indigenous Concrete Printer and advanced AI technologies. Sustainability and circular economy principles should be integrated into the project to reduce the construction industry's carbon footprint. Continued research and innovation in 3D concrete printing, AI, and construction materials will keep the project at the forefront of technological advancements and industry trends.

In summary, by embracing large-scale implementation, advancing AI technologies, and emphasizing sustainability and innovation, the Development of Indigenous Concrete Printer and Mix Design project can transform the construction industry.

References

3D Printing of Houses Mexico. (n.d.). Retrieved June 27, 2023, from https://interestingengineering.com/innovation/this-entire-village-was-built-by-a-single-3d-printer

Aïtcin, P.-C. (2000). Cements of yesterday and today: concrete of tomorrow. *Cement and Concrete Research*, *30*(9), 1349–1359.

Alexander, M., & Mindess, S. (2005). *Aggregates in concrete*. CRC Press.

Almazrouei, A., Susantyoko, R. A., Wu, C.-H., Mustafa, I., Alhammadi, A., & Almheiri, S. (2019). Robust Surface-Engineered Tape-Cast and Extrusion Methods to Fabricate Electrically-Conductive Poly(vinylidene fluoride)/Carbon Nanotube Filaments for Corrosion-Resistant 3D Printing Applications. *Scientific Reports*, *9*(1), 9618. https://doi.org/10.1038/s41598-019-45992-5

Altaf, M. A., Whittington, D., Jamal, H., & Smith, V. K. (1993). Rethinking rural water supply policy in the Punjab, Pakistan. *Water Resources Research*, *29*(7), 1943–1954.

Andrew Ting, G. H., Noel Quah, T. K., Lim, J. H., Daniel Tay, Y. W., & Tan, M. J. (2022). Extrudable region parametrical study of 3D printable concrete using recycled glass concrete. *Journal of Building Engineering*, *50*, 104091. https://doi.org/10.1016/J.JOBE.2022.104091

Assaad, J., Khayat, K. H., & Mesbah, H. (2003). Variation of formwork pressure with thixotropy of self-consolidating concrete. *Materials Journal*, *100*(1), 29–37.

Babar, M. S., Tazyeen, S., Khan, H., Tsagkaris, C., Essar, M. Y., & Ahmad, S. (2021). Impact of climate change on health in Karachi, Pakistan. *The Journal of Climate Change and Health*, *2*, 100013.

Bagheri, A., & Cremona, C. (2020). Formulation of mix design for 3D printing of geopolymers: A machine learning approach. *Materials Advances*, *1*(4), 720–727.

Balletti, C., Ballarin, M., & Guerra, F. (2017). 3D printing: State of the art and future perspectives. *Journal of Cultural Heritage*. https://doi.org/10.1016/j.culher.2017.02.010

Barnes, H. A. (1997). Thixotropy—a review. *Journal of Non-Newtonian Fluid Mechanics*, *70*(1), 1–33. https://doi.org/https://doi.org/10.1016/S0377-0257(97)00004-9

Baz, B., Remond, S., & Aouad, G. (2022). Influence of the mix composition on the thixotropy of 3D printable mortars. *Magazine of Concrete Research*, *74*(6), 271–283.

Bhattacherjee, S., Basavaraj, A. S., Rahul, A. V, Santhanam, M., Gettu, R., Panda, B., Schlangen, E., Chen, Y., Copuroglu, O., Ma, G., Wang, L., Basit Beigh, M. A., & Mechtcherine, V. (2021). Sustainable materials for 3D concrete printing. *Cement and Concrete Composites*, *122*, 104156. https://doi.org/https://doi.org/10.1016/j.cemconcomp.2021.104156

Bhattacherjee, S., & Santhanam, M. (2020). Enhancing Buildability of 3D Printable Concrete by Spraying of Accelerating Admixture on Surface. In F. P. Bos, S. S. Lucas, R. J. M. Wolfs, & T. A. M. Salet (Eds.), *Second RILEM International Conference on Concrete and Digital Fabrication* (pp. 13–22). Springer International Publishing.

Bolshakova, V., Guerriero, A., & Halin, G. (2018). Identification of relevant project documents to 4D BIM uses for a synchronous collaborative decision support. *Creative Construction Conference 2018*, 1036–1043.

Boral, P. (2019). The design of the CNC milling machine. *MATEC Web of Conferences*, *254*, 01003.

Bos, F. P., Bosco, E., & Salet, T. A. M. (2019). Ductility of 3D printed concrete reinforced with short straight steel fibers. *Virtual and Physical Prototyping*, *14*(2), 160–174. https://doi.org/10.1080/17452759.2018.1548069

Brescia-Norambuena, L., Gonzalez, M., Avudaiappan, S., Flores, E. I. S., & Grasley, Z. (2021). Improving concrete underground mining pavements performance through the synergic effect of silica fume, nanosilica, and polypropylene fibers. *Construction and Building Materials*, *285*, 122895.

Buswell, R. A., Leal de Silva, W. R., Jones, S. Z., & Dirrenberger, J. (2018). 3D printing using concrete extrusion: A roadmap for research. *Cement and Concrete Research*, *112*, 37–49. https://doi.org/10.1016/J.CEMCONRES.2018.05.006

Butkutė, K., & Vaitkevičius, V. (2023). 3D concrete printing with wastes for building applications. *Journal of Physics: Conference Series*, *2423*(1), 012034.
Cao, X., Yu, S., Cui, H., & Li, Z. (2022). 3D Printing Devices and Reinforcing Techniques for Extruded Cement-Based Materials: A Review. *Buildings*, *12*(4), 453.
Chandra, S., & Björnström, J. (2002). Influence of superplasticizer type and dosage on the slump loss of Portland cement mortars—Part II. *Cement and Concrete Research*, *32*(10), 1613–1619. https://doi.org/https://doi.org/10.1016/S0008-8846(02)00838-4
Chen, H., Zhang, D., Chen, P., Li, N., & Perrot, A. (2023). A Review of the Extruder System Design for Large-Scale Extrusion-Based 3D Concrete Printing. *Materials*, *16*(7), 2661.
Chen, J., Liu, X., Tian, Y., Zhu, W., Yan, C., Shi, Y., Kong, L. B., Qi, H. J., & Zhou, K. (2022). 3D-Printed Anisotropic Polymer Materials for Functional Applications. *Advanced Materials*, *34*(5), 2102877. https://doi.org/https://doi.org/10.1002/adma.202102877
Chen, M., Li, L., Zheng, Y., Zhao, P., Lu, L., & Cheng, X. (2018). Rheological and mechanical properties of admixtures modified 3D printing sulphoaluminate cementitious materials. *Construction and Building Materials*, *189*, 601–611. https://doi.org/https://doi.org/10.1016/j.conbuildmat.2018.09.037
Chen, M., Yang, L., Zheng, Y., Huang, Y., Li, L., Zhao, P., Wang, S., Lu, L., & Cheng, X. (2020). Yield stress and thixotropy control of 3D-printed calcium sulfoaluminate cement composites with metakaolin related to structural build-up. *Construction and Building Materials*, *252*, 119090.
Chen, M., Yang, L., Zheng, Y., Li, L., Wang, S., Huang, Y., Zhao, P., Lu, L., & Cheng, X. (2021). Rheological behaviors and structure build-up of 3D printed polypropylene and polyvinyl alcohol fiber-reinforced calcium sulphoaluminate cement composites. *Journal of Materials Research and Technology*, *10*, 1402–1414. https://doi.org/https://doi.org/10.1016/j.jmrt.2020.12.115
Chen, T., He, T., Benesty, M., Khotilovich, V., Tang, Y., Cho, H., Chen, K., Mitchell, R., Cano, I., & Zhou, T. (2015). Xgboost: extreme gradient boosting. *R Package Version 0.4-2*, *1*(4), 1–4.
Chen, Y., Zhang, Y., Pang, B., Liu, Z., & Liu, G. (2021). Extrusion-based 3D printing concrete with coarse aggregate: Printability and direction-dependent mechanical performance. *Construction and Building Materials*, *296*, 123624. https://doi.org/10.1016/J.CONBUILDMAT.2021.123624
Cho, S., Kruger, P. J., Zeranka, S., & Van Zijl, G. (2019). 3D printable concrete technology and mechanics. *Concrete Beton*, *158*, 11–18.
Chong, L., Ramakrishna, S., & Singh, S. (2018). A review of digital manufacturing-based hybrid additive manufacturing processes. *The International Journal of Advanced Manufacturing Technology*, *95*(5), 2281–2300. https://doi.org/10.1007/s00170-017-1345-3
Chu, S. H., Yang, E. H., & Unluer, C. (2023). Development of nanofiber reinforced reactive magnesia-based composites for 3D printing. *Construction and Building Materials*, *366*, 130270. https://doi.org/10.1016/J.CONBUILDMAT.2022.130270
Das, A., Song, Y., Mantellato, S., Wangler, T., Flatt, R. J., & Lange, D. A. (2020). Influence of pumping/extrusion on the air-void system of 3D printed concrete. *Second RILEM International Conference on Concrete and Digital Fabrication: Digital Concrete 2020 2*, 417–427.
Dauji, S. (2016). Prediction of compressive strength of concrete with decision trees. *International Journal of Concrete Technology*, *2*(1), 19–29.
De Schutter, G., Lesage, K., Mechtcherine, V., Nerella, V. N., Habert, G., & Agusti-Juan, I. (2018). Vision of 3D printing with concrete—Technical, economic and environmental potentials. *Cement and Concrete Research*, *112*, 25–36.
Dilawar Riaz, R., Usman, M., Ali, A., Majid, U., Faizan, M., & Jalil Malik, U. (2023). Inclusive characterization of 3D printed concrete (3DPC) in additive manufacturing: A detailed review. *Construction and Building Materials*, *394*, 132229. https://doi.org/https://doi.org/10.1016/j.conbuildmat.2023.132229
Ding, T., Xiao, J., Zou, S., & Wang, Y. (2020). Hardened properties of layered 3D printed concrete with recycled sand. *Cement and Concrete Composites*, *113*, 103724.
Ding, T., Xiao, J., Zou, S., & Zhou, X. (2020). Anisotropic behavior in bending of 3D printed concrete reinforced with fibers. *Composite Structures*, *254*, 112808.

https://www.sciencedirect.com/science/article/pii/S0263822320327343
Dwinugroho, T. B., Kumarajati, D. Y. H., & Hapsari, Y. T. (2019). Design and implementation of CNC (computer numerical control) based automatic stamp batik machine program with automatic gripper using Mach 3. *Journal of Physics: Conference Series*, *1254*(1), 012069.
Dwivedi, A., Pal, A., Patel, S. S., Chourasia, A., & Jain, A. K. (2022). Evaluation of Model 3D Printer and Design Mix for 3D Concrete Printing. In *Advances in Construction Materials and Sustainable Environment* (pp. 837–847). Springer.
Ebden, M. (2015). Gaussian processes: A quick introduction. *ArXiv Preprint ArXiv:1505.02965*.
Faes, M., Valkenaers, H., Vogeler, F., Vleugels, J., & Ferraris, E. (2015). Extrusion-based 3D printing of ceramic components. *Procedia Cirp*, *28*, 76–81.
Friedman, J. H. (2001). Greedy function approximation: a gradient boosting machine. *Annals of Statistics*, 1189–1232.
Gjørv, O. E. (2008). High-strength concrete. In *Developments in the Formulation and Reinforcement of Concrete* (pp. 153–170). Elsevier.
Goldin, M. (2014). Chinese Company Builds Houses Quickly With 3D Printing. *Mashable. Com, April*, *29*.
González-Taboada, I., González-Fonteboa, B., Martínez-Abella, F., & Seara-Paz, S. (2018). Thixotropy and interlayer bond strength of self-compacting recycled concrete. *Construction and Building Materials*, *161*, 479–488. https://doi.org/10.1016/J.CONBUILDMAT.2017.11.157
Gordon, S., & Hillery, M. T. (2005). Development of a high-speed CNC cutting machine using linear motors. *Journal of Materials Processing Technology*, *166*(3), 321–329.
Grigoriev, S. N., & Martinov, G. M. (2018). An approach to creation of terminal clients in CNC system. *2018 3rd Russian-Pacific Conference on Computer Technology and Applications (RPC)*, 1–4.
Gupta, S. M. (2007). Support vector machines based modelling of concrete strength. *World Academy of Science, Engineering and Technology*, *36*.
Hasan, A., & Arif, H. (2018). *Pakistan: the causes and repercussions of the housing crisis*.
Hasan, M. M., Khan, M. R., Noman, A. T., Rashid, H., Ahmed, N., & Reza, S. M. T. (2019a). Design and implementation of a microcontroller based low cost computer numerical control (CNC) plotter using motor driver controller. *2019 International Conference on Electrical, Computer and Communication Engineering (ECCE)*, 1–5.
Hasan, M. M., Khan, M. R., Noman, A. T., Rashid, H., Ahmed, N., & Reza, S. M. T. (2019b). Design and implementation of a microcontroller based low cost computer numerical control (CNC) plotter using motor driver controller. *2019 International Conference on Electrical, Computer and Communication Engineering (ECCE)*, 1–5.
Heras Murcia, D., Genedy, M., & Reda Taha, M. M. (2020). Examining the significance of infill printing pattern on the anisotropy of 3D printed concrete. *Construction and Building Materials*, *262*, 120559. https://doi.org/10.1016/J.CONBUILDMAT.2020.120559
Hou, S., Duan, Z., Xiao, J., & Ye, J. (2021a). A review of 3D printed concrete: Performance requirements, testing measurements and mix design. *Construction and Building Materials*, *273*, 121745. https://doi.org/https://doi.org/10.1016/j.conbuildmat.2020.121745
Hou, S., Duan, Z., Xiao, J., & Ye, J. (2021b). A review of 3D printed concrete: Performance requirements, testing measurements and mix design. *Construction and Building Materials*, *273*, 121745. https://doi.org/https://doi.org/10.1016/j.conbuildmat.2020.121745
Jabeen, A., Sheng, H. X., & Aamir, M. (2015). Housing crises in Pakistan: Review of population growth and deficiencies in housing laws and policies. *International Journal of Sciences: Basic and Applied Research*, *24*(3), 323–347.
Jayachandraiah, B., Krishna, O. V., Khan, P. A., & Reddy, R. A. (2014). Fabrication of low cost 3-Axis CNC router. *International Journal of Engineering Science Invention*, *3*(6), 1–10.
Jayathilakage, R., Rajeev, P., & Sanjayan, J. G. (2020). Yield stress criteria to assess the buildability of 3D concrete printing. *Construction and Building Materials*, *240*, 117989.
Jeong, H., Han, S.-J., Choi, S.-H., Lee, Y. J., Yi, S. T., & Kim, K. S. (2019). Rheological property criteria

for buildable 3D printing concrete. *Materials*, *12*(4), 657.
Jiang, Q., Liu, Q., Wu, S., Zheng, H., & Sun, W. (2022). Modification effect of nanosilica and polypropylene fiber for extrusion-based 3D printing concrete: printability and mechanical anisotropy. *Additive Manufacturing*, 102944.
Jiao, D., De Schryver, R., Shi, C., & De Schutter, G. (2021). Thixotropic structural build-up of cement-based materials: A state-of-the-art review. *Cement and Concrete Composites*, *122*, 104152. https://doi.org/10.1016/J.CEMCONCOMP.2021.104152
Jo, J. H., Jo, B. W., Cho, W., & Kim, J.-H. (2020). Development of a 3D printer for concrete structures: laboratory testing of cementitious materials. *International Journal of Concrete Structures and Materials*, *14*(1), 1–11.
Joh, C., Lee, J., Bui, T. Q., Park, J., & Yang, I.-H. (2020a). Buildability and Mechanical Properties of 3D Printed Concrete. In *Materials* (Vol. 13, Issue 21). https://doi.org/10.3390/ma13214919
Joh, C., Lee, J., Bui, T. Q., Park, J., & Yang, I.-H. (2020b). Buildability and mechanical properties of 3D printed concrete. *Materials*, *13*(21), 4919.
Kaliyavaradhan, S. K., Ambily, P. S., Prem, P. R., & Ghodke, S. B. (2022). Test methods for 3D printable concrete. *Automation in Construction*, *142*, 104529. https://doi.org/https://doi.org/10.1016/j.autcon.2022.104529
Kamali, M., & Hewage, K. (2017). Development of performance criteria for sustainability evaluation of modular versus conventional construction methods. *Journal of Cleaner Production*, *142*, 3592–3606.
Karyne Levy. (2014, April 15). *A Chinese Company 3-D Printed 10 Houses In A Day*.
Kazemian, A., Yuan, X., Cochran, E., & Khoshnevis, B. (2017). Cementitious materials for construction-scale 3D printing: Laboratory testing of fresh printing mixture. *Construction and Building Materials*, *145*, 639–647. https://doi.org/10.1016/J.CONBUILDMAT.2017.04.015
Keating, J., & Hannant, D. J. (1989). The effect of rotation rate on gel strength and dynamic yield strength of thixotropic oil well cements measured using a shear vane. *Journal of Rheology*, *33*(7), 1011–1020.
Kecman, V. (2005). Support vector machines–an introduction. In *Support vector machines: theory and applications* (pp. 1–47). Springer.
Khayat, K. H., Kassimi, F., & Ghoddousi, P. (2014). Mixture design and testing of fiber-reinforced self-consolidating concrete. *ACI Materials Journal*, *111*(2), 143.
Khayat, K. H., Saric-Coric, M., & Liotta, F. (2002). Influence of thixotropy on stability characteristics of cement grout and concrete. *Materials Journal*, *99*(3), 234–241.
Kim, D. M. (2013). Contour crafting: a future method of building. *Illumin Article, Writing*, *340*.
Kingsford, C., & Salzberg, S. L. (2008). What are decision trees? *Nature Biotechnology*, *26*(9), 1011–1013.
Kosmatka, S. H., Kerkhoff, B., Panarese, W. C., MacLeod, N. F., & McGrath, R. J. (2002). Designing and proportioning normal concrete mixtures. *Design and Control of Concrete Mixtures. Portland Cement Association*, 151–172.
Kotsiantis, S. B. (2013). Decision trees: a recent overview. *Artificial Intelligence Review*, *39*, 261–283.
Kumar, M. A., Krishnaraj, J., & Reddy, R. (2017a). Mini CNC 2D sketcher for accurate building drawing. *International Journal of Civil Engineering and Technology*, *8*(6), 543–549.
Kumar, M. A., Krishnaraj, J., & Reddy, R. (2017b). Mini CNC 2D sketcher for accurate building drawing. *International Journal of Civil Engineering and Technology*, *8*(6), 543–549.
Lao, W., Li, M., Masia, L., & Tan, M. J. (2017). Approaching rectangular extrudate in 3D printing for building and construction by experimental iteration of nozzle design. *2017 International Solid Freeform Fabrication Symposium*.
Lao, W., Li, M., & Tjahjowidodo, T. (2021). Variable-geometry nozzle for surface quality enhancement in 3D concrete printing. *Additive Manufacturing*, *37*, 101638. https://doi.org/https://doi.org/10.1016/j.addma.2020.101638
Lediga, R., & Kruger, D. (2017). Optimizing concrete mix design for application in 3D printing

technology for the construction industry. *Solid State Phenomena*, *263*, 24–29.
Liu, J., Setunge, S., & Tran, P. (2022). 3D concrete printing with cement-coated recycled crumb rubber: Compressive and microstructural properties. *Construction and Building Materials*, *347*, 128507. https://doi.org/10.1016/J.CONBUILDMAT.2022.128507
Liu, J., & Tran, P. (2022). Experimental study on 3D-printed cementitious materials containing surface-modified recycled crumb rubber. *Materials Today: Proceedings*. https://doi.org/10.1016/J.MATPR.2022.08.550
Liu, Z., Li, M., Weng, Y., Wong, T. N., & Tan, M. J. (2019). Mixture Design Approach to optimize the rheological properties of the material used in 3D cementitious material printing. *Construction and Building Materials*, *198*, 245–255. https://doi.org/https://doi.org/10.1016/j.conbuildmat.2018.11.252
Lu, B., Weng, Y., Li, M., Qian, Y., Leong, K. F., Tan, M. J., & Qian, S. (2019). A systematical review of 3D printable cementitious materials. *Construction and Building Materials*, *207*, 477–490. https://doi.org/10.1016/J.CONBUILDMAT.2019.02.144
M., J. A. (2016). Effect of Buildability on Labor Productivity: A Practical Quantification Approach. *Journal of Construction Engineering and Management*, *142*(2), 6015002. https://doi.org/10.1061/(ASCE)CO.1943-7862.0001062
Ma, G., Li, Z., Wang, L., Wang, F., & Sanjayan, J. (2019). Mechanical anisotropy of aligned fiber reinforced composite for extrusion-based 3D printing. *Construction and Building Materials*, *202*, 770–783. https://doi.org/https://doi.org/10.1016/j.conbuildmat.2019.01.008
Ma, G., Salman, N. M., Wang, L., & Wang, F. (2020). A novel additive mortar leveraging internal curing for enhancing interlayer bonding of cementitious composite for 3D printing. *Construction and Building Materials*, *244*, 118305. https://doi.org/10.1016/J.CONBUILDMAT.2020.118305
Ma, S., Yang, H., Zhao, S., He, P., Zhang, Z., Duan, X., Yang, Z., Jia, D., & Zhou, Y. (2021). 3D-printing of architectured short carbon fiber-geopolymer composite. *Composites Part B: Engineering*, *226*, 109348. https://doi.org/10.1016/J.COMPOSITESB.2021.109348
Madekar, K. J., Nanaware, K. R., Phadtare, P. R., & Mane, V. S. (2016). Automatic mini CNC machine for PCB drawing and drilling. *International Research Journal of Engineering and Technology (IRJET)*, *3*(02), 1107–1108.
Magnel, G., & Zollman, C. C. (1954). *Prestressed concrete*. McGraw-Hill New York.
Manikandan, K., Wi, K., Zhang, X., Wang, K., & Qin, H. (2020). Characterizing cement mixtures for concrete 3D printing. *Manufacturing Letters*, *24*, 33–37.
Marchment, T., & Sanjayan, J. (2019). Method of Enhancing Interlayer Bond Strength in 3D Concrete Printing. In T. Wangler & R. J. Flatt (Eds.), *First RILEM International Conference on Concrete and Digital Fabrication – Digital Concrete 2018* (pp. 148–156). Springer International Publishing.
Marczyk, J., Ziejewska, C., Gądek, S., Korniejenko, K., Łach, M., Góra, M., Kurek, I., Doğan-Sağlamtimur, N., Hebda, M., & Szechyńska-Hebda, M. (2021). Hybrid materials based on fly ash, metakaolin, and cement for 3D printing. *Materials*, *14*(22), 6874.
Marijnissen, M., & Van Der Zee, A. (2017). 3D Concrete printing in architecture. *A Research on the Potential Benefits of 3D Concrete Printing in Architecture. Material Studies–Methodologies*, *2*, 299–308.
McGee, W., Ng, T. Y., Yu, K., & Li, V. C. (2020). Extrusion Nozzle Shaping for Improved 3DP of Engineered Cementitious Composites (ECC/SHCC). In F. P. Bos, S. S. Lucas, R. J. M. Wolfs, & T. A. M. Salet (Eds.), *Second RILEM International Conference on Concrete and Digital Fabrication* (pp. 916–925). Springer International Publishing.
Mohan, M. K., Rahul, A. V, van Dam, B., Zeidan, T., De Schutter, G., & Van Tittelboom, K. (2022). Performance criteria, environmental impact and cost assessment for 3D printable concrete mixtures. *Resources, Conservation and Recycling*, *181*, 106255.
Mohtasham Moein, M., Saradar, A., Rahmati, K., Ghasemzadeh Mousavinejad, S. H., Bristow, J., Aramali, V., & Karakouzian, M. (2023). Predictive models for concrete properties using machine learning and deep learning approaches: A review. *Journal of Building Engineering*, *63*, 105444. https://doi.org/10.1016/J.JOBE.2022.105444

Møller, P. C. F., Mewis, J., & Bonn, D. (2006). Yield stress and thixotropy: on the difficulty of measuring yield stresses in practice. *Soft Matter*, *2*(4), 274–283.
Montepio, R. C. (2009). Optimizing the Soil Auger Blade on Clay Loam Soil. *Southeastern Philippines Journal of Research and Development*, *18*(2), 1.
Mori, K., Akita, K., & Abe, Y. (2007). Springback behaviour in bending of ultra-high-strength steel sheets using CNC servo press. *International Journal of Machine Tools and Manufacture*, *47*(2), 321–325.
Muthukrishnan, S., Ramakrishnan, S., & Sanjayan, J. (2021a). Technologies for improving buildability in 3D concrete printing. *Cement and Concrete Composites*, *122*, 104144.
Muthukrishnan, S., Ramakrishnan, S., & Sanjayan, J. (2021b). Technologies for improving buildability in 3D concrete printing. *Cement and Concrete Composites*, *122*, 104144.
Muthukrishnan, S., Ramakrishnan, S., & Sanjayan, J. (2021c). Technologies for improving buildability in 3D concrete printing. *Cement and Concrete Composites*, *122*, 104144.
Muthukrishnan, S., Ramakrishnan, S., & Sanjayan, J. (2022). Set on demand geopolymer using print head mixing for 3D concrete printing. *Cement and Concrete Composites*, *128*, 104451.
Nadimalla, A. M., Masjuki, S. A., Saad, S. A., & Ali, M. (2022). Machine Learning Model to Predict Slump, VEBE and Compaction Factor of M Sand and Shredded Pet Bottles Concrete. *IOP Conference Series: Materials Science and Engineering*, *1244*(1), 012023.
Nae, I., & Andrei, T. (2010). Designing and Building a CNC Router Using Stepper Motors. *Petroleum-Gas University of Ploiesti Bulletin, Technical Series*, *62*(1).
Nerella, V. N., Beigh, M. A. B., Fataei, S., & Mechtcherine, V. (2019). Strain-based approach for measuring structural build-up of cement pastes in the context of digital construction. *Cement and Concrete Research*, *115*, 530–544. https://doi.org/10.1016/J.CEMCONRES.2018.08.003
Nerella, V. N., Näther, M., Iqbal, A., Butler, M., & Mechtcherine, V. (2019). Inline quantification of extrudability of cementitious materials for digital construction. *Cement and Concrete Composites*, *95*, 260–270. https://doi.org/https://doi.org/10.1016/j.cemconcomp.2018.09.015
Ngo, T. D., Kashani, A., Imbalzano, G., Nguyen, K. T. Q., & Hui, D. (2018). Additive manufacturing (3D printing): A review of materials, methods, applications and challenges. *Composites Part B: Engineering*, *143*, 172–196. https://doi.org/https://doi.org/10.1016/j.compositesb.2018.02.012
Nguyen, H., Vu, T., Vo, T. P., & Thai, H. T. (2021). Efficient machine learning models for prediction of concrete strengths. *Construction and Building Materials*, *266*, 120950. https://doi.org/10.1016/J.CONBUILDMAT.2020.120950
Nguyen-Sy, T., Wakim, J., To, Q.-D., Vu, M.-N., Nguyen, T.-D., & Nguyen, T.-T. (2020). Predicting the compressive strength of concrete from its compositions and age using the extreme gradient boosting method. *Construction and Building Materials*, *260*, 119757. https://doi.org/https://doi.org/10.1016/j.conbuildmat.2020.119757
Omidinasab, F., Sahraei Moghadam, A., & Dowlatshahi, M. B. (2022a). Predictive model for shear strength estimation in reinforced concrete beams with recycled aggregates using Gaussian process regression. *Neural Computing and Applications*, 1–17.
Omidinasab, F., Sahraei Moghadam, A., & Dowlatshahi, M. B. (2022b). Predictive model for shear strength estimation in reinforced concrete beams with recycled aggregates using Gaussian process regression. *Neural Computing and Applications*, 1–17.
Panda, B., Chandra Paul, S., & Jen Tan, M. (2017). Anisotropic mechanical performance of 3D printed fiber reinforced sustainable construction material. *Materials Letters*, *209*, 146–149. https://doi.org/10.1016/J.MATLET.2017.07.123
Panda, B., Noor Mohamed, N. A., Tay, Y. W. D., & Tan, M. J. (2018). Bond strength in 3D printed geopolymer mortar. *RILEM International Conference on Concrete and Digital Fabrication*, 200–206.
Panda, B., Paul, S. C., Mohamed, N. A. N., Tay, Y. W. D., & Tan, M. J. (2018). Measurement of tensile bond strength of 3D printed geopolymer mortar. *Measurement*, *113*, 108–116. https://doi.org/10.1016/J.MEASUREMENT.2017.08.051

Panda, B., Tay, Y. W. D., Paul, S. C., & Tan, M. J. (2018a). Current challenges and future potential of 3D concrete printing. *Materialwissenschaft Und Werkstofftechnik*, *49*(5), 666–673. https://doi.org/https://doi.org/10.1002/mawe.201700279

Panda, B., Tay, Y. W. D., Paul, S. C., & Tan, M. J. (2018b). Current challenges and future potential of 3D concrete printing. *Materialwissenschaft Und Werkstofftechnik*, *49*(5), 666–673. https://doi.org/https://doi.org/10.1002/mawe.201700279

Papachristoforou, M., Mitsopoulos, V., & Stefanidou, M. (2018). Evaluation of workability parameters in 3D printing concrete. *Procedia Structural Integrity*, *10*, 155–162.

Patel, N. (2020). Study on computer numerical control (CNC) technology. *Int. Res. J. Eng. Technol.(IRJET)*, *7*, 2883–2887.

Puzatova, A., Shakor, P., Laghi, V., & Dmitrieva, M. (2022). Large-Scale 3D Printing for Construction Application by Means of Robotic Arm and Gantry 3D Printer: A Review. *Buildings*, *12*(11), 2023.

Different Effects of NSF and PCE Superplasticizer on Adsorption, Dynamic Yield Stress and Thixotropy of Cement Pastes, 11 Materials 695 (2018). https://doi.org/10.3390/ma11050695

Qian, Y., Lesage, K., El Cheikh, K., & De Schutter, G. (2018). Effect of polycarboxylate ether superplasticizer (PCE) on dynamic yield stress, thixotropy and flocculation state of fresh cement pastes in consideration of the Critical Micelle Concentration (CMC). *Cement and Concrete Research*, *107*, 75–84.

Quatrano, A., De, S., Rivera, Z. B., & Guida, D. (2017). Development and implementation of a control system for a retrofitted CNC machine by using Arduino. *FME Transactions*, *45*(4), 565–571.

Rahmatullah, R., Amiruddin, A., & Lubis, S. (2021). Effectiveness of CNC Turning and CNC Milling in Machining Process. *International Journal of Economic, Technology and Social Sciences (Injects)*, *2*(2), 575–583.

Rahul, A. V., Mohan, M. K., De Schutter, G., & Van Tittelboom, K. (2022). 3D printable concrete with natural and recycled coarse aggregates: Rheological, mechanical and shrinkage behaviour. *Cement and Concrete Composites*, *125*, 104311. https://doi.org/10.1016/J.CEMCONCOMP.2021.104311

Rahul, A. V., & Santhanam, M. (2020). Evaluating the printability of concretes containing lightweight coarse aggregates. *Cement and Concrete Composites*, *109*, 103570. https://doi.org/10.1016/J.CEMCONCOMP.2020.103570

Rahul, A. V, Santhanam, M., Meena, H., & Ghani, Z. (2019). 3D printable concrete: Mixture design and test methods. *Cement and Concrete Composites*, *97*, 13–23.

Rasheed, A., Usman, M., Farooq, H., & Hanif, A. (2018). Effect of Super-plasticizer Dosages on Fresh State Properties and Early-Age Strength of Concrete. *IOP Conference Series: Materials Science and Engineering*, *431*(6), 062010. https://doi.org/10.1088/1757-899X/431/6/062010

Rehman, A., & Jamil, F. (2021). Impact of urban residential location choice on housing, travel demands and associated costs: Comparative analysis with empirical evidence from Pakistan. *Transportation Research Interdisciplinary Perspectives*, *10*, 100357.

Rehman, A. U., & Kim, J.-H. (2021). 3D Concrete Printing: A Systematic Review of Rheology, Mix Designs, Mechanical, Microstructural, and Durability Characteristics. In *Materials* (Vol. 14, Issue 14). https://doi.org/10.3390/ma14143800

Rehman, F., Khokhar, S. A., & Khushnood, R. A. (2022). ANN based predictive mimicker for mechanical and rheological properties of eco-friendly geopolymer concrete. *Case Studies in Construction Materials*, *17*, e01536.

Rollakanti, C. R., & Prasad, C. V. S. R. (2022). Applications, performance, challenges and current progress of 3D concrete printing technologies as the future of sustainable construction–A state of the art review. *Materials Today: Proceedings*.

Roussel, N. (2018). Rheological requirements for printable concretes. *Cement and Concrete Research*, *112*, 76–85. https://doi.org/10.1016/J.CEMCONRES.2018.04.005

Sahin, H. G., & Mardani, A. (2022a). SUSTAINABLE 3D PRINTING CONCRETE MIXTURES. *Journal of Modern Technology and Engineering*, *7*(1), 20–29.

Sahin, H. G., & Mardani, A. (2022b). SUSTAINABLE 3D PRINTING CONCRETE MIXTURES.

Journal of Modern Technology and Engineering, *7*(1), 20–29.
Salet, T. A. M., & Wolfs, R. J. M. (2016). Potentials and challenges in 3D concrete printing. *2nd International Conference on Progress in Additive Manufacturing (Pro-Am 2016), May 16-19 2016, Singapore*, 8–13.
Sanjayan, J. G., & Nematollahi, B. (2019). 3D concrete printing for construction applications. In *3D concrete printing technology* (pp. 1–11). Elsevier.
Sanjayan, J. G., Nematollahi, B., Xia, M., & Marchment, T. (2018). Effect of surface moisture on inter-layer strength of 3D printed concrete. *Construction and Building Materials*, *172*, 468–475. https://www.sciencedirect.com/science/article/pii/S0950061818307384
Sarker, I. H. (2021). Machine learning: Algorithms, real-world applications and research directions. *SN Computer Science*, *2*(3), 160.
Secrieru, E., Fataei, S., Schröfl, C., & Mechtcherine, V. (2017). Study on concrete pumpability combining different laboratory tools and linkage to rheology. *Construction and Building Materials*, *144*, 451–461. https://doi.org/https://doi.org/10.1016/j.conbuildmat.2017.03.199
Shakor, P., Nejadi, S., Paul, G., Sanjayan, J., & Nazari, A. (2019). Mechanical properties of cement-based materials and effect of elevated temperature on three-dimensional (3-D) printed mortar specimens in inkjet 3-D printing. *ACI Materials Journal*, *116*(2), 55–67.
Słoński, M. (2011). Bayesian neural networks and Gaussian processes in identification of concrete properties. *Computer Assisted Methods in Engineering and Science*, *18*(4), 291–302.
Soltan, D. G., & Li, V. C. (2018). A self-reinforced cementitious composite for building-scale 3D printing. *Cement and Concrete Composites*, *90*, 1–13. https://doi.org/10.1016/J.CEMCONCOMP.2018.03.017
Sonebi, M., Cevik, A., Grünewald, S., & Walraven, J. (2016). Modelling the fresh properties of self-compacting concrete using support vector machine approach. *Construction and Building Materials*, *106*, 55–64. https://doi.org/10.1016/J.CONBUILDMAT.2015.12.035
Srinivas, D., Dey, D., Panda, B., & Sitharam, T. G. (2022a). Printability, Thermal and Compressive Strength Properties of Cementitious Materials: A Comparative Study with Silica Fume and Limestone. *Materials*, *15*(23), 8607.
Srinivas, D., Dey, D., Panda, B., & Sitharam, T. G. (2022b). Printability, Thermal and Compressive Strength Properties of Cementitious Materials: A Comparative Study with Silica Fume and Limestone. *Materials*, *15*(23), 8607.
Sulaiman, T. M. S. T., Minhat, M., Mohamed, S. B., Mohamed, A. S., Mohamed, A. R., & Yusof, S. N. A. (2020). File and PC-Based CNC Controller using Integrated Interface System (I2S). *Journal of Advanced Research in Applied Mechanics*, *70*(1), 1–8.
Taffese, W., Sistonen, E., & Puttonen, J. A. (2015). Prediction of concrete carbonation depth using decision trees. *ESANN*.
Tay, Y. W. D., Qian, Y., & Tan, M. J. (2019a). Printability region for 3D concrete printing using slump and slump flow test. *Composites Part B: Engineering*, *174*, 106968.
Tay, Y. W. D., Qian, Y., & Tan, M. J. (2019b). Printability region for 3D concrete printing using slump and slump flow test. *Composites Part B: Engineering*, *174*, 106968.
Tripathi, A., Nair, S. A. O., & Neithalath, N. (2022). A comprehensive analysis of buildability of 3D-printed concrete and the use of bi-linear stress-strain criterion-based failure curves towards their prediction. *Cement and Concrete Composites*, *128*, 104424.
UN-Habitat - A Better Urban Future | UN-Habitat. (n.d.). Retrieved August 1, 2023, from https://unhabitat.org/
Uppala, S. S., & Tadikamalla, M. R. (2017). A review on 3D printing of concrete-the future of sustainable construction. *I-Manager's Journal on Civil Engineering*, *7*(3), 49.
Valkenaers, H., Jansen, D., Voet, A., Van Gysel, A., & Ferraris, E. (2014). Additive manufacturing for concrete: A 3D printing principle. *Proceedings of the 14th Euspen International Conference*, *1*, 139–142.
Van Den Bergh, J., Nieuw, C., Slob, W., Escalante Suarez, M., & Velema, P. Lou. (n.d.). *Modular 3D*

printing construction: towards affordable, adjustable and climate-resilient housing.
Van Der Putten, J., De Schutter, G., & Van Tittelboom, K. (2019). Surface modification as a technique to improve inter-layer bonding strength in 3D printed cementitious materials. *RILEM Technical Letters*, *4*(0), 33–38. https://doi.org/10.21809/rilemtechlett.2019.84
Van Der Putten, J., Rahul, A. V., De Schutter, G., & Van Tittelboom, K. (2021). Development of 3D printable cementitious composites with the incorporation of polypropylene fibers. *Materials*, *14*(16), 4474.
Wang, X., Jia, L., Jia, Z., Zhang, C., Chen, Y., Ma, L., Wang, Z., Deng, Z., Banthia, N., & Zhang, Y. (2022). Optimization of 3D printing concrete with coarse aggregate via proper mix design and printing process. *Journal of Building Engineering*, *56*, 104745. https://doi.org/10.1016/J.JOBE.2022.104745
Wolfs, R. J. M., & Suiker, A. S. J. (2019). Structural failure during extrusion-based 3D printing processes. *The International Journal of Advanced Manufacturing Technology*, *104*(1), 565–584. https://doi.org/10.1007/s00170-019-03844-6
Wongkornchaowalit, N., & Lertchirakarn, V. (2011). Setting Time and Flowability of Accelerated Portland Cement Mixed with Polycarboxylate Superplasticizer. *Journal of Endodontics*, *37*(3), 387–389. https://doi.org/https://doi.org/10.1016/j.joen.2010.11.039
Wu, B.-Y., & Hsu, P.-L. (2015). Robust controller design for CNC servo motors against the variation of external loading via the H∞/QFT approach. *2015 IEEE International Conference on Advanced Intelligent Mechatronics (AIM)*, 1467–1471.
Wu, Y.-C., & Li, M. (2022). Effects of Early-Age rheology and printing time interval on Late-Age fracture characteristics of 3D printed concrete. *Construction and Building Materials*, *351*, 128559.
Xu, J., Chen, M., Zhao, Z., Li, L., Wang, S., Huang, Y., Zhao, P., Gong, C., Lu, L., & Cheng, X. (2021). Printability and efflorescence control of admixtures modified 3D printed white Portland cement-based materials based on the response surface methodology. *Journal of Building Engineering*, *38*, 102208. https://doi.org/10.1016/J.JOBE.2021.102208
Xu, J., Ding, L., Cai, L., Zhang, L., Luo, H., & Qin, W. (2019). Volume-forming 3D concrete printing using a variable-size square nozzle. *Automation in Construction*, *104*, 95–106. https://doi.org/https://doi.org/10.1016/j.autcon.2019.03.008
Yan, K., & Shi, C. (2010). Prediction of elastic modulus of normal and high strength concrete by support vector machine. *Construction and Building Materials*, *24*(8), 1479–1485. https://doi.org/10.1016/J.CONBUILDMAT.2010.01.006
Yang, H., & Che, Y. (2022). Recycling of aggregate micro fines as a partial replacement for fly ash in 3D printing cementitious materials. *Construction and Building Materials*, *321*, 126372.
Yang, L., Sepasgozar, S. M. E. E., Shirowzhan, S., Kashani, A., & Edwards, D. (2023). Nozzle criteria for enhancing extrudability, buildability and interlayer bonding in 3D printing concrete. *Automation in Construction*, *146*, 104671. https://doi.org/10.1016/J.AUTCON.2022.104671
Yao, X., Luan, C., Zhang, D., Lan, L., & Fu, J. (2017). Evaluation of carbon fiber-embedded 3D printed structures for strengthening and structural-health monitoring. *Materials & Design*, *114*, 424–432. https://doi.org/10.1016/J.MATDES.2016.10.078
Yu, K., McGee, W., Ng, T. Y., Zhu, H., & Li, V. C. (2021). 3D-printable engineered cementitious composites (3DP-ECC): Fresh and hardened properties. *Cement and Concrete Research*, *143*, 106388. https://doi.org/10.1016/J.CEMCONRES.2021.106388
Yu, S., Du, H., & Sanjayan, J. (2020). Aggregate-bed 3D concrete printing with cement paste binder. *Cement and Concrete Research*, *136*, 106169. https://doi.org/10.1016/J.CEMCONRES.2020.106169
Zareiyan, B., & Khoshnevis, B. (2017). Effects of interlocking on interlayer adhesion and strength of structures in 3D printing of concrete. *Automation in Construction*, *83*, 212–221. https://doi.org/10.1016/J.AUTCON.2017.08.019
Zhang, C., Jia, Z., Wang, X., Jia, L., Deng, Z., Wang, Z., Zhang, Y., & Mechtcherine, V. (2022). A two-phase design strategy based on the composite of mortar and coarse aggregate for 3D printable

concrete with coarse aggregate. *Journal of Building Engineering*, *54*, 104672. https://doi.org/10.1016/J.JOBE.2022.104672

Zhang, C., Nerella, V. N., Krishna, A., Wang, S., Zhang, Y., Mechtcherine, V., & Banthia, N. (2021). Mix design concepts for 3D printable concrete: A review. *Cement and Concrete Composites*, *122*, 104155. https://doi.org/https://doi.org/10.1016/j.cemconcomp.2021.104155

Zhang, J., Wang, J., Dong, S., Yu, X., & Han, B. (2019). A review of the current progress and application of 3D printed concrete. *Composites Part A: Applied Science and Manufacturing*, *125*, 105533. https://doi.org/https://doi.org/10.1016/j.compositesa.2019.105533

Zhang, J., Wang, P., & Gao, R. X. (2019). Deep learning-based tensile strength prediction in fused deposition modeling. *Computers in Industry*, *107*, 11–21. https://doi.org/https://doi.org/10.1016/j.compind.2019.01.011

Zhang, Y., Zhang, Y., She, W., Yang, L., Liu, G., & Yang, Y. (2019). Rheological and harden properties of the high-thixotropy 3D printing concrete. *Construction and Building Materials*, *201*, 278–285. https://www.sciencedirect.com/science/article/pii/S0950061818330356

Zhao, Y., Wu, X., Zhu, L., Yang, Z., Wang, Y., & Xi, X. (2021). The influence of polypropylene fiber on the working performance and mechanical anisotropy of 3d printing concrete. *Journal of Advanced Concrete Technology*, *19*(12), 1264–1274.

Zhao, Y., Yang, G., Zhu, L., Ding, Y., Guan, X., Wu, X., & Yang, Z. (2022). Effects of rheological properties and printing speed on molding accuracy of 3D printing basalt fiber cementitious materials. *Journal of Materials Research and Technology*, *21*, 3462–3475. https://www.sciencedirect.com/science/article/pii/S2238785422016623

Zheng, J., Zhang, M., & Meng, Q. (2006). Modeling and design of servo system of CNC machine tools. *2006 International Conference on Mechatronics and Automation*, 1964–1969.

Zhou, Y., Jiang, D., Sharma, R., Xie, Y. M., & Singh, A. (2023). Enhancement of 3D printed cementitious composite by short fibers: A review. *Construction and Building Materials*, *362*, 129763. https://doi.org/https://doi.org/10.1016/j.conbuildmat.2022.129763

Zou, S., Xiao, J., Ding, T., Duan, Z., & Zhang, Q. (2021). Printability and advantages of 3D printing mortar with 100% recycled sand. *Construction and Building Materials*, *273*, 121699. https://doi.org/10.1016/J.CONBUILDMAT.2020.121699